NAVAL POSTGRADUATE SCHOOL
Monterey, California

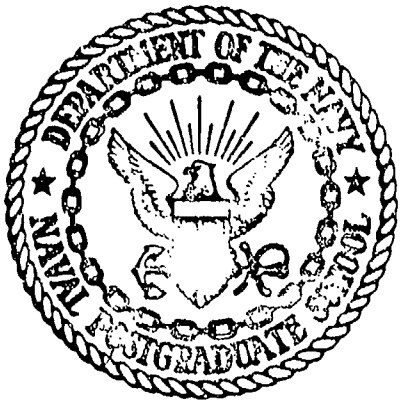

THESIS

Probability of Intercept in
Electronic Countermeasures Receivers

by

Barry Frederick Schwoerer

December 1975

Thesis Advisor: S. Jauregui, Jr.

UNCLASSIFIED

SECURITY CLASSIFICATION OF THIS PAGE (When Data Entered)

REPORT DOCUMENTATION PAGE		READ INSTRUCTIONS BEFORE COMPLETING FORM
1. REPORT NUMBER	2. GOVT ACCESSION NO.	3. RECIPIENT'S CATALOG NUMBER
4. TITLE (and Subtitle) Probability of Intercept in Electronic Countermeasures Receivers		5. TYPE OF REPORT & PERIOD COVERED Master's Thesis; December 1975 6. PERFORMING ORG. REPORT NUMBER
7. AUTHOR(s) Barry Frederick Schwoerer		8. CONTRACT OR GRANT NUMBER(s)
9. PERFORMING ORGANIZATION NAME AND ADDRESS Naval Postgraduate School Monterey, California 93940		10. PROGRAM ELEMENT, PROJECT, TASK AREA & WORK UNIT NUMBERS
11. CONTROLLING OFFICE NAME AND ADDRESS Naval Postgraduate School Monterey, California 93940		12. REPORT DATE December 1975 13. NUMBER OF PAGES 122
14. MONITORING AGENCY NAME & ADDRESS (if different from Controlling Office) Naval Postgraduate School Monterey, California 93940		15. SECURITY CLASS. (of this report) UNCLASSIFIED 15a. DECLASSIFICATION/DOWNGRADING SCHEDULE

16. DISTRIBUTION STATEMENT (of this Report)

Approved for public release; distribution unlimited

17. DISTRIBUTION STATEMENT (of the abstract entered in Block 20, if different from Report)

18. SUPPLEMENTARY NOTES

19. KEY WORDS (Continue on reverse side if necessary and identify by block number)

Probability of intercept	IFM receiver	Probability of detection
ECM receivers	Acoustooptic receiver	Threshold detection
Receiver scan rates	Two-tuple receiver	Noise figure
Effective bandwidth	Signal density	Noise temperature

20. ABSTRACT (Continue on reverse side if necessary and identify by block number)

Modern electronic warfare systems are directed against an ever increasing variety of electronic systems. It is necessary to intercept certain signals so that countermeasures or analysis can be accomplished. To accomplish the intercept, receiving systems with as high a probability of intercept as possible are required. This study examines factors causing probability of intercept to decrease and the methods that may be used to combat those factors. Receiving systems having unity probability of intercept are examined. Systems examined

DD FORM 1 JAN 73 1473 (Page 1)

EDITION OF 1 NOV 65 IS OBSOLETE

S/N 0102-014-6601

UNCLASSIFIED

SECURITY CLASSIFICATION OF THIS PAGE (When Data Ente

are the IFM, acoustooptic and two-tuple type receiver. The effects of external and internal noise, receiver and antenna scan factors, signal density, signal processors, display systems and bandwidth are factors limiting probability of intercept that are examined. One concludes that through proper design, systems can be achieved with unity intercept probability.

Probability of Intercept in

Electronic Countermeasures Receivers

by

Barry Frederick Schwoerer
Lieutenant, United States Navy
B. S., San Jose State University, 1968

Submitted in partial fulfillment of the
requirements for the degree of

MASTER OF SCIENCE IN ELECTRICAL ENGINEERING

from the

NAVAL POSTGRADUATE SCHOOL
December 1975

Author 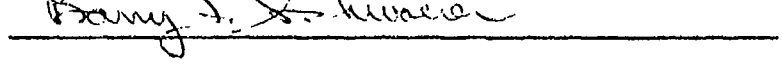

Approved by: 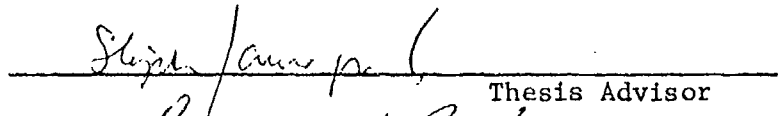
Thesis Advisor

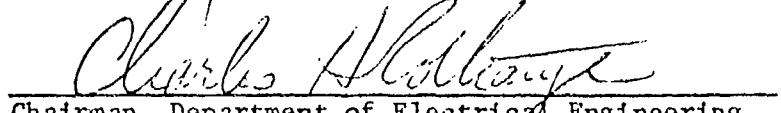
Chairman, Department of Electrical Engineering

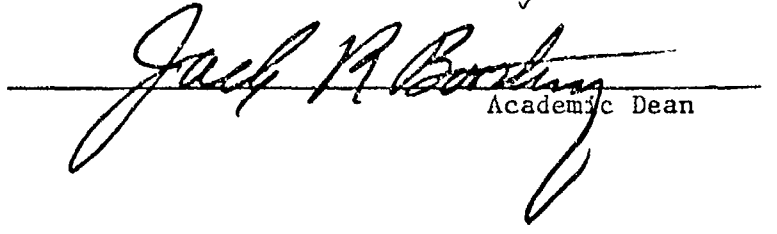
Academic Dean

ABSTRACT

Modern electronic warfare systems are directed against an ever increasing variety of electronic systems. It is necessary to intercept certain signals so that countermeasures or analysis can be accomplished. To accomplish the intercept, receiving systems with as high a probability of intercept as possible are required. This study examines factors causing probability of intercept to decrease and the methods that may be used to combat those factors. Receiving systems having unity probability of intercept are examined. Systems examined are the IFM, acoustooptic and two-tuple type receiver. The effects of external and internal noise, receiver and antenna scan factors, signal density, signal processors, display systems and bandwidth are factors limiting probability of intercept that are examined. One concludes that through proper design, systems can be achieved with unity intercept probability.

TABLE OF CONTENTS

LIST OF TABLES

LIST OF FIGURES

I. INTRODUCTION

In modern warfare, the electronic war is an ever increasing factor in determining the outcome. Intelligence gathering systems must intercept signals of interest so that electronic orders of battle can be produced. Countermeasures systems must intercept signals so that countermeasures can be applied to weapons systems actively engaging the countermeasures platform. In both cases, the ability of the system to perform its function is directly related to the probability that the signal of interest will be received and detected. Ideally the probability of a success is unity. One finds that several factors cause a reduction in the probability of intercept (POI). Section II defines POI and states the problem to be analyzed in the remainder of this report. Section III presents factors and methods to overcome those factors that work to decrease POI. The fundamental factor limiting POI is the probability of detection (P_d) where P_d is a function of noise. Noise and its affect on intercept systems is presented in Section III. Section IV examines methods used to improve POI by overcoming some of the factors outlined in Section III. Section V examines systems with unity POI including the two-tuple channelized receiver, instantaneous frequency measuring (IFM) receiver, and the acoustooptic receiver. Difficulties encountered in the employment of the receivers are discussed.

II. PROBLEM STATEMENT

ECM intercept systems are designed with the goal to intercept electronic signals of interest to collect information on the facilities, capabilities, and intentions of a potential or actual enemy. [1] It is essential to the success of a countermeasures operation to obtain knowledge of the possible presence of an enemy as early as possible. To this end, equipment with a high intercept probability coupled with rapid signal acquisition is necessary. [2] The probability that a given signal is detected and processed by the system is defined as the probability of intercept (POI). POI is a function of both the signal and receiver system. Ideally, the intercept system should intercept any signal emitted whose range is less than maximum range based on free space attenuation factors and the sensitivity of the system. The ideal system would have high sensitivity, low probability of false alarm, wide rf bandwidth, 360° antenna coverage, ability to direction find to a high degree of accuracy, large processing capacity, be reliable, economical, and have a POI of unity. Obviously a single receiver meeting the requirements listed does not exist. Design of an ECM intercept system then becomes a trade-off of the various factors outlined.

To analyze ECM systems considering POI one must understand that POI is largely a matter of definition based on the purpose of the particular system. It is unnecessary to specify unity probability of intercept simply because it is the ideal case. To do so may require a system of greater complexity than is required to accomplish the mission. It is more

realistic to specify POI based on working backwards from the maximum time allowable before intercept or time to identification in automatic systems. "Mini" computers and special purpose Electronic Warfare processors such as Applied Technology's ATAC 8 are able to process signal pulse trains over a period of many pulses without requiring unity probability of intercept on every pulse. By processing over many pulses the system behaves analogous to radar systems where the receiver integrates several pulses to improve detectability. It is sufficient in other systems to simply intercept a fraction of the total signal emitted in order to display or alarm the presence of a signal. In still other systems it is necessary to intercept every pulse. In all cases, POI may be defined as unity if the system completes the mission for which it is designed.

A main difficulty in attempting to obtain unity single-pulse probability of intercept is the "through-time" of the system. Through-time is defined as the time required for a signal to travel from the receiver antenna terminal to the final output device. Through-time can be especially troublesome in automated systems where buffering, storage, and logic networks are encountered; all of which increase through-time. An excessive through-time serves to create a traffic jam at the output of the analog-to-digital converter. Methods used to alleviate this problem will be covered in a later section.

Signal characteristics are not under the control of the designer; therefore, the system must be designed so as to minimize the effect of signal parameters. Signal parameters affecting the design are the antenna

scan characteristics, effective radiated power (ERP) modulation type and the transmitter duty cycle. Antenna scan characteristics affect the total time the transmitter looks in the direction of the intercept system. The ERP is a function of transmitter power and antenna gain and affects the distance at which the signal is detectable by the receiver. Transmitter duty cycle is defined as the ratio of pulse width to pulse repetition interval and is a measure of the percentage of time energy is emitted from the transmitter. The methods used to analyze a particular situation and determine the POI of a system are the subject of the following section.

III. FACTORS AFFECTING PROBABILITY OF INTERCEPT

A. RECEIVER NOISE CONSIDERATIONS

1. General Noise Discussion

In the absence of noise, there would be no degradation of signal quality and one would need only gain to overcome transmission losses. Noise can mask weak signals and create uncertainty in others. [5] Random noise arises from several sources, including external radiation, noise generated internally called Johnson or thermal noise, shot noise from vacuum devices, transistor noise and equivalent noise sources such as lossy elements that contribute effective noise powers. This random noise is characterized as wideband with a uniform (flat) spectral density and Gaussian amplitude probability distribution

2. External Noise

At radio frequencies, noise enters a system through the antenna from certain external sources. Noise emanates from any object above absolute zero (zero degrees Kelvin). Objects at or near the earth's surface are nominally at a noise temperature of 290°K. Objects in space and in the atmosphere contribute varying noise temperatures. Below 10 MHz, the majority of the sky noise comes from atmospheric noise generated by lightning and atmospheric disturbances. Through VHF (Bands A & B) and UHF (Bands C & D) the major contributor becomes cosmic noise, or noise generated from objects in space external to the atmosphere. Included here are the sun, moon, stars and galactic noise, with the galactic noise predominant. The galactic plane as observed on earth displays many

discrete sources and groupings of sources that constitute a sky map.[7] Directional antennas can examine these "hot spots" on the sky map as well as the cooler sections of deep space void of stellar objects. This results in a very wide variation in noise power received as one scans the sky. Most antennas in the UHF and VHF region are not particularly directive, looking at a much wider section of sky at one time. If one integrates the contribution of each source covered by the intercept area of the antenna one obtains an overall sky temperature. This sky temperature will vary from night to day, time of the year and position on earth. Figure 1 illustrates experimentally determined curves for sky temperature as a representative average of upper and lower extremes. As frequency is increased, galactic effect diminishes and noise due to atmospheric water and oxygen absorption becomes more significant. Above approximately 10 GHz resonance effects in CO_2, O_2 and water vapor contribute alternate "windows" and absorption bands in the atmosphere.[9] Oliver's report [8] is an excellent system noise study with examples in UHF, VHF and SHF and tables useful for system noise calculations. Atmospheric noise temperature decreases as elevation angle increases from the horizon, and is a function of weather. [5]

3. Internal Noise

An ECM system's probability of intercept is fundamentally limited to a value less than unity by noise. Noise entering a receiver or generated within a receiver sets the signal-to-noise level required to achieve design probability of detection and probability of false alarm.

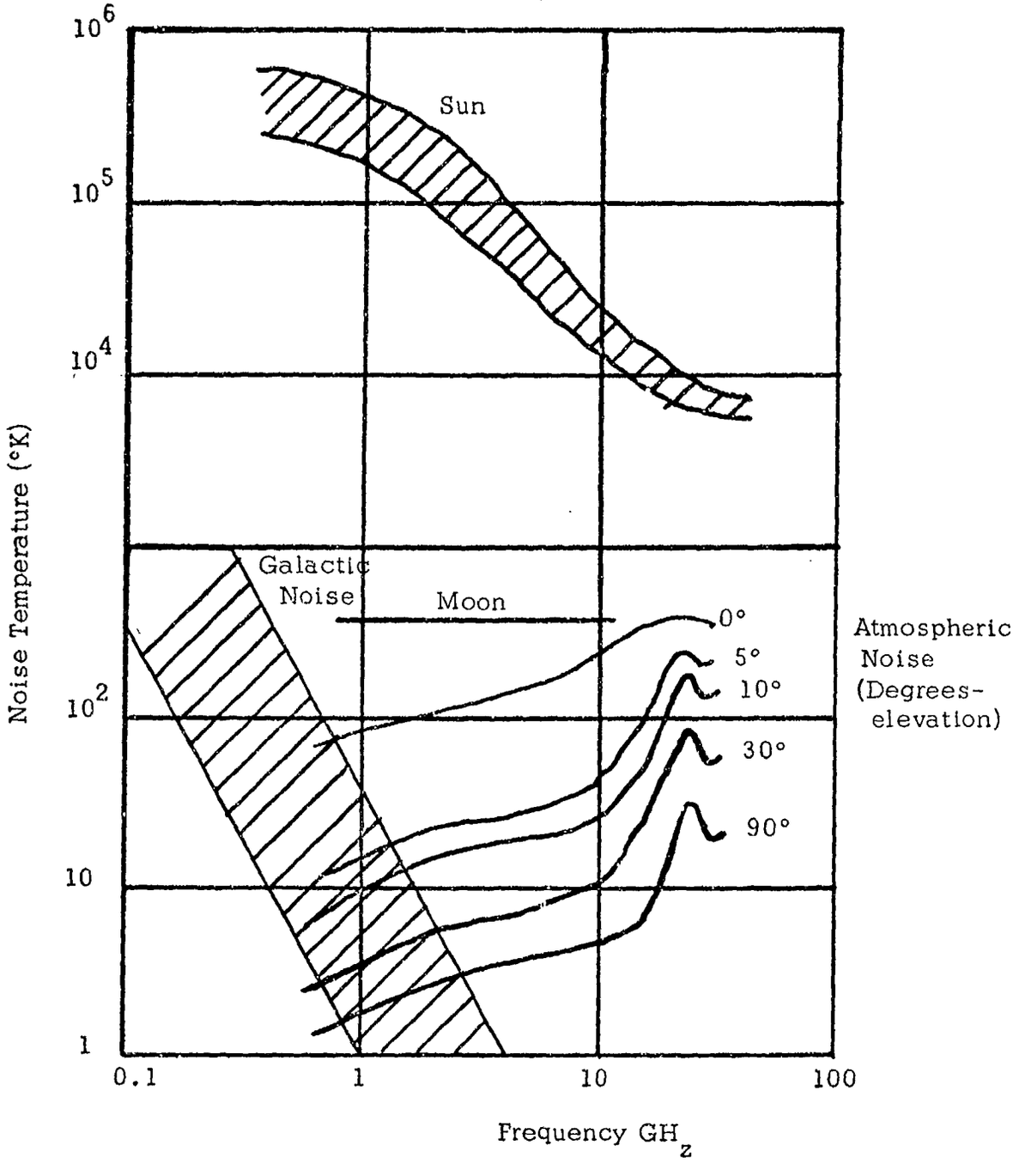

Figure 1. Galactic and Atmospheric Noise Versus Frequency

For this reason it is important to review the sources of noise in a typical ECM system and the methods commonly used to describe this noise.

From a noise standpoint an ECM system consists of the antenna, amplifier, and detector, where the amplifier and detector constitute the receiver. The antenna is considered as a device which reflects its radiation resistance at the input of the receiver into a thermal reservoir contained in that portion of space observed by the antenna. If one considered the observed medium to be a composite black body at temperature T the radiation resistance of the antenna will come into equilibrium with the temperature of this reservoir. The power input to the amplifier is then Johnson noise power. This power is equivalent to the power output of a resistor matched to the receiver input and immersed in a thermal reservoir at temperature T. In the discussion that follows, noise temperature will be used instead of noise figure to describe system noise response.

The advantage of using noise temperature vice noise figure is twofold. First, consistent units can be used for comparing antenna noise with other noise generated in the system, and second, the overall system sensitivity can be obtained which will include antenna noise. For example let T_s be the system noise temperature approximated by

$$T_s = T_a + T_f + T_r \qquad (2)$$

where T_a is the antenna noise temperature, T_f is the antenna feed and cabling equivalent noise temperature, and T_r is the receiver noise temperature considering all components that follow the receiver. [5]

Noise figure was originally developed to deal with relatively noisy early radar and ECM receivers. Modern low noise devices are more suited to a noise description using equivalent noise temperature. [6] Noise figure and noise temperature both describe the same property of a receiver but at different ends of the temperature spectrum. It will be demonstrated later in this report that significant errors can result from the incorrect choice of method for noise calculations.

When portions of a system absorb energy (losses), one must be able to convert those losses to an equivalent noise temperature. The noise output of a lossy element is the attenuated noise input plus Johnson noise generated by the device due to a temperature increase resulting from the absorption of power. Appendix A contains an example of a typical calculation for the determination of equivalent noise temperature for a lossy device.

4. Noise Figure Versus Noise Temperature

When calculating receiver sensitivity it is common practice for engineers to use an approximate equation for noise power at receiver input, $N=kT_oBG$, where T_o is the reference temperature 290°K, k is Boltzmann's constant, B the receiver bandwidth in Hz, and F the receiver noise figure. This formula gives sufficient accuracy when noise powers are 10 dB or greater, or is accurate to within one percent provided $|F(GHz)| / |T(°K)| \leq 0.2$, where F is the frequency at which noise power is calculated. [10, 7]

Many systems are much better than 10 dB noise. It will be demonstrated that errors as great as 10 dB can result by using the approximate formula.

As illustrated in Appendix B the exact value of Johnson noise in a resistor R at temperature T is given by $N=4T_e \Delta F$ where T_e is the equivalent noise temperature, and ΔF the noise bandwidth. Using the approximate equation for noise power one can demonstrate (App. B) that $N=k \Delta F(T_o + T_e)$. Taking the ratio of the approximate and exact result leads to an error expressed in dB of

$$\text{Error (dB)} = 10 \log_{10}\left(1 + \frac{T_o}{T_e}\right) \tag{3}$$

Figure 2 illustrates the result. From the curve it is apparent that if receiver noise figure is less than 5 dB the error is significant. [10] The figure demonstrates that the use of noise temperature is preferred over noise figure when working with low noise systems. It should be noted that the noise sensitivity calculated using the approximate equation will always be on the conservative side, hence its popularity. For most calculations a conservative result is preferred compared to an over optimistic result which may be unattainable in practice.

5. Probability of Detection and Probability of False Alarm

a. Background

The weakest signal a receiver can detect is the minimum detectable signal, S_{min}. Detection is based on establishing a threshold level at the output of the receiver. If the receiver output exceeds threshold it is assumed that a signal is present. This method of detection is

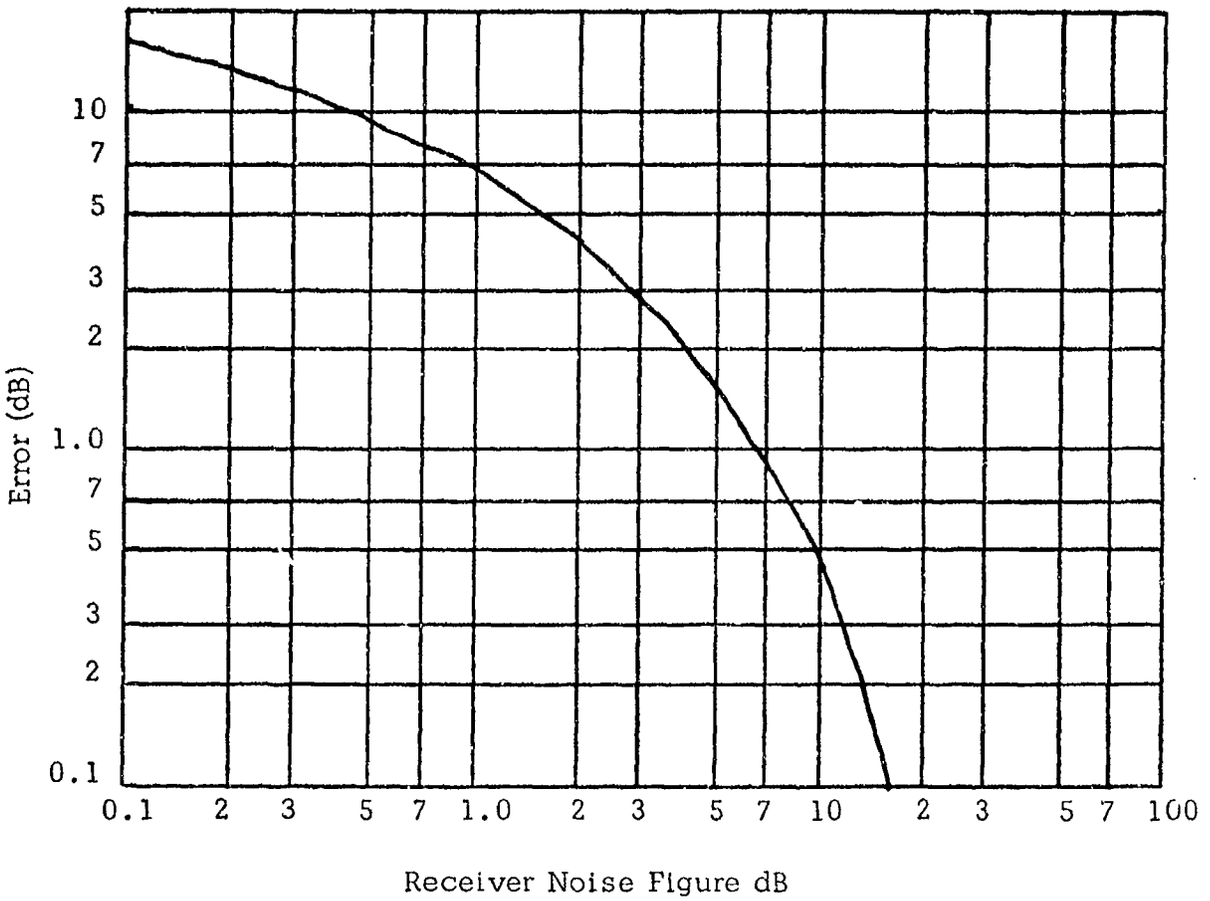

Figure 2. Noise Power Approximation Versus Noise Figure

called threshold detection. With threshold detection, any time a signal input falls within the receiver pass band and has sufficient intensity a signal interception will be made. Thus with threshold detection probability of intercept becomes the probability of coincidence between the signal parameters; signal strength, frequency, and time of arrival, and the receiver parameters; threshold voltage V_t, bandwidth and scan characteristics.[1] For broadband systems with omnidirectional antennas, the calculation of the probability of intercept is reduced to calculating the percentage of time the signal input exceeds the receiver threshold. Due to the nature of noise described in the previous section the process of detection is not a linear function but is statistical in nature. Further, the threshold level must be low if weak signals are to be detected, but it cannot be so low that noise peaks cross the threshold to give false indications of the presence of signals. [9]

The noise power at the receiver input is kTB_n where B_n is the noise bandwidth defined as the bandwidth of an idealized (rectangular) filter which passes the same noise power as does the real filter. B_n is given as

$$B_n = \frac{\int_{-\infty}^{\infty} |H(f)|^2 \, df}{|H(f_o)|^2} \tag{4}$$

where: H(f) = frequency response of the IF amplifier

f_o = frequency of maximum response

In most receivers the 3 dB bandwidth and B_n do not differ appreciably. Table 2.1 of reference 9 compares various filter types.

Using equation (B-4) and (B-5), and solving for S_i,

$$S_i = F_n S_o K T_o B_n / N_o \tag{5}$$

where: F_n = noise figure of receiver

S_o = output signal power

B_n = noise bandwidth

N_o = noise output power

If S_{min} is that value of S_i corresponding to the minimum signal-to-noise ratio for detection, then S_{min} is given by

$$S_{min} = K T_o B_n F_n (S_o/N_o)_{min} \tag{6}$$

The purpose of this derivation is to show the minimum detectable signal for a specified $(S_o/N_o)_{min}$. $(S_o/N_o)_{min}$ will be obtained as a result of the calculation for the probability of detection. S_{min} can then be used in the one-way range equation

$$S_{min} = \frac{P_t G_t}{4\pi R^2} \tag{7}$$

to calculate the maximum range from target emitter that will still allow detection at the receiver.

b. Probability of False Alarm

In ECM receivers similar to that illustrated in .gure 3 probability of false alarm is calculated assuming the input to be noise only.

The second detector and video amplifier are assumed to form an envelope detector, that is, one which rejects the carrier frequency

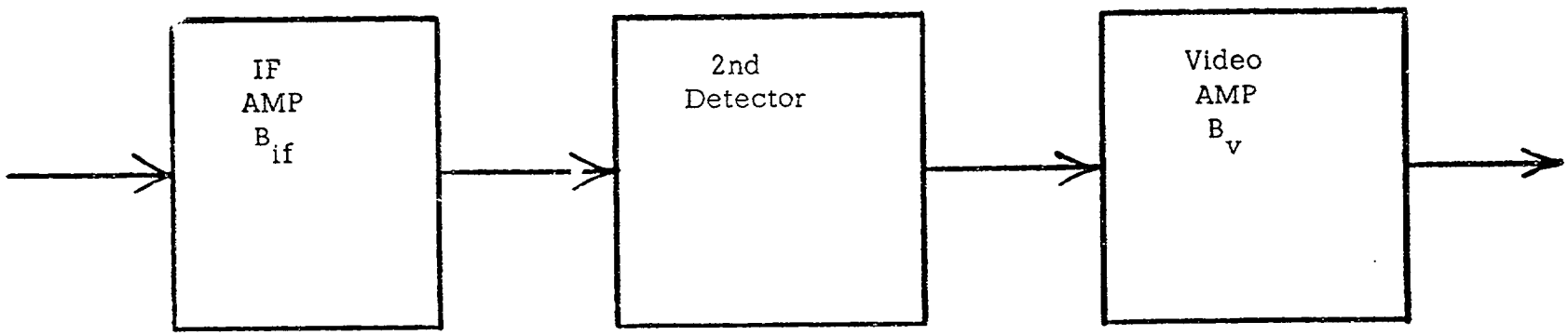

Figure 3. Typical Simple ECM Receiver

but passes the modulation envelope. Either a square-law or linear detector may be assumed since the effect on the probability of detection by assuming one instead of the other is small. [9]

Assuming the input noise to be Gaussian one can show (Ap$_r$. C) that the probability of false alarm is given by

$$P_{fa} = \exp\left(-V_t^2/2\psi_o\right) \tag{8}$$

The value $V_t^2/2\ \psi_o$ in equation (8) is the signal voltage to noise voltage ratio, using the threshold voltage V_t.

Threshold detection is selected so as not to exceed a specified false alarm probability, that is, the probability of detection is maximized for a fixed probability of false alarm. This is equivalent to fixing the probability of type I error which occurs when noise exceeds the threshold creating a false alarm, and minimizes type II error which occurs when noise reduces signal below threshold for a missed detection. Threshold detection then is equivalent to the Neyman-Pearson test used in statistics for determining the validity of a specified hypothesis. [9] The Neyman-Pearson criterion provides the uniformly most powerful statistically based test for obtaining an indication of when a signal exceeds threshold. Tests other than Neyman-Pearson lead to a higher probability of error for a given signal-to-noise ratio. [9, 17] The Neyman-Pearson criterion is well suited to ECM receiver work since it directly leads into probability of detection and probability of false alarm discussions. Whether one realizes it or not, the Neyman-Pearson criterion is used in most ECM receiver design work.

From Johnson's work, equation (B-1) one notes that the noise power is proportional to bandwidth. It follows therefore that the number of times per second that noise crosses the threshold is proportional to bandwidth and that the time between false alarms if given by, $T_{fa} = 1/P_{fa}B_{if}$, where B_{if} is the i-f bandwidth. Substituting equation (8) into P_{fa} one obtains

$$T_{fa} = \frac{1}{B_{if}\ \exp(-V_t^2/2\psi_o)} \tag{9}$$

Equation (9) is plotted in Figure 4, with $V_t^2/2\psi_o$ as the abscissa.

Probability of false alarm is important in ECM receivers since every false alarm is displayed as an intercept. In systems utilizing mini-computers for signal sorting and identification it is necessary to limit the input data rate to a level such that processing can be accomplished without excessive buffering. Excessive false alarms generate unnecessary input data degrading the processors ability to sort and identify signals of interest. The effects of system P_{fa} on the overall performance of an ECM system was analyzed in a paper by J. E. Nicholson [18] where he makes use of Baye's conditional probability theorem. [19] Nicholson demonstrated that threat warning systems require a P_{fa} much greater than 1×10^{-4} in order to avoid excessive signal classification errors.

c. Probability of Detection

When signal is added to Gaussian noise the sum of the two signals is a Gaussian variable with non-zero mean. The process of determining when the signal exceeds threshold is illustrated in Appendix D where the probability that a signal will be detected is shown to be given by

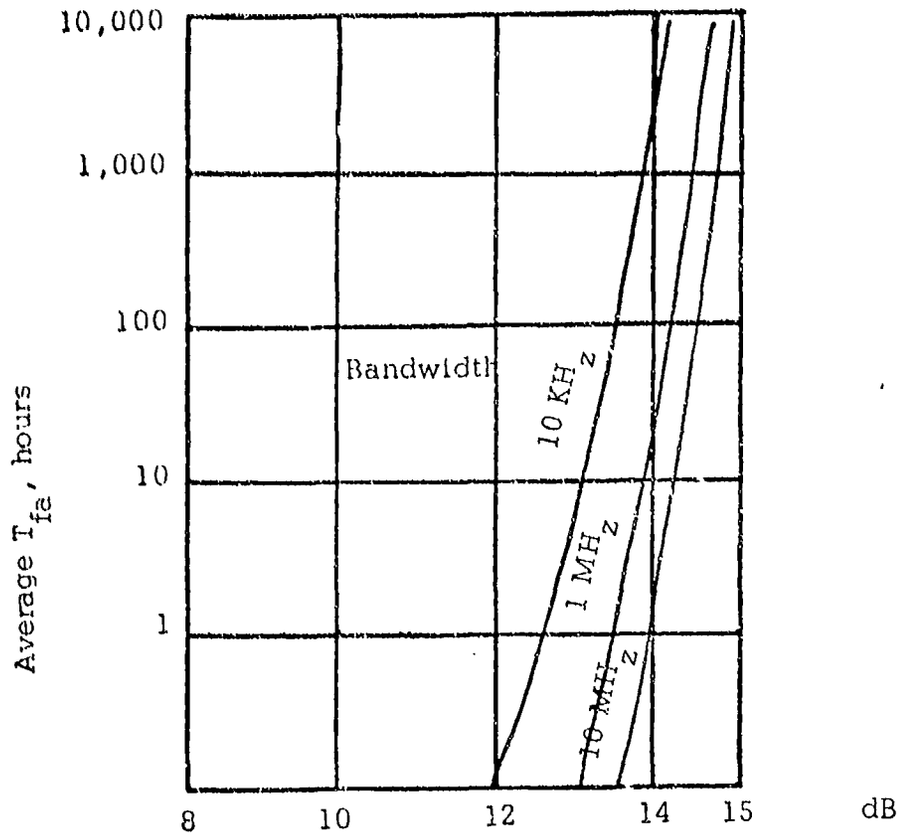

Figure 4. T_{fa} as a Function of V_t and Bandwidth

$$P_d \approx \frac{1}{2}\left(1 - \operatorname{erf}\frac{V_t - A}{\sqrt{2\psi_o}}\right) + \frac{\exp\left[\frac{-(V_t-A)^2}{2\psi_o}\right]}{2\sqrt{2\pi}\left(\frac{A}{\psi_o}\right)}\left[1 - \frac{V_t - A}{4A} + \frac{1+(V_t-A)^2\psi_o}{\frac{8A^2}{\psi_o}} - \cdots\right] \quad (10)$$

Equation (10) can be used to plot a family of curves relating P_d to V_t and the input signal A. Since most engineers prefer to work with signal-to-noise power ratios, $A/\sqrt{\psi_o}$ can be converted to a power ratio by noting that

$$\frac{A}{\sqrt{\psi_o}} = \frac{\sqrt{2}\,(\text{rms signal voltage})}{\text{rms noise voltage}} = \frac{(2\text{ signal power})^{1/2}}{\text{noise power}} = \left(\frac{2S}{N}\right)^{1/2}$$

For ease in plotting the curves replace $V_t^2/2\,\psi_o$ in equation (10) by $\ln(1/P_{fa})$. Figure 5 plots equation (10) as a function of P_{fa} and S/N.[9]

Signal-to-noise is obtained from Figure 5 after the designer has selected the probability of detection and probability of false alarm desired. The value of S/N obtained is used in equation (6) to determine S_{min}. S_{min} is then used to determine the maximum range from target emitter that will still allow detection by the system. By utilizing equation (7) and solving for R, where R is the range from target emitter to receiver, one can obtain R_{max}.

Macnee, et. al. [1] utilize a definition of P_d similar to equation (10) but prefer to use a detectability index, d, vice signal-to-noise ratio, where for an excatly known signal, d is defined as

$$d = \frac{2E}{N_o} = \frac{2S\tau}{N} B = (S/N)\,2B\tau \quad (11)$$

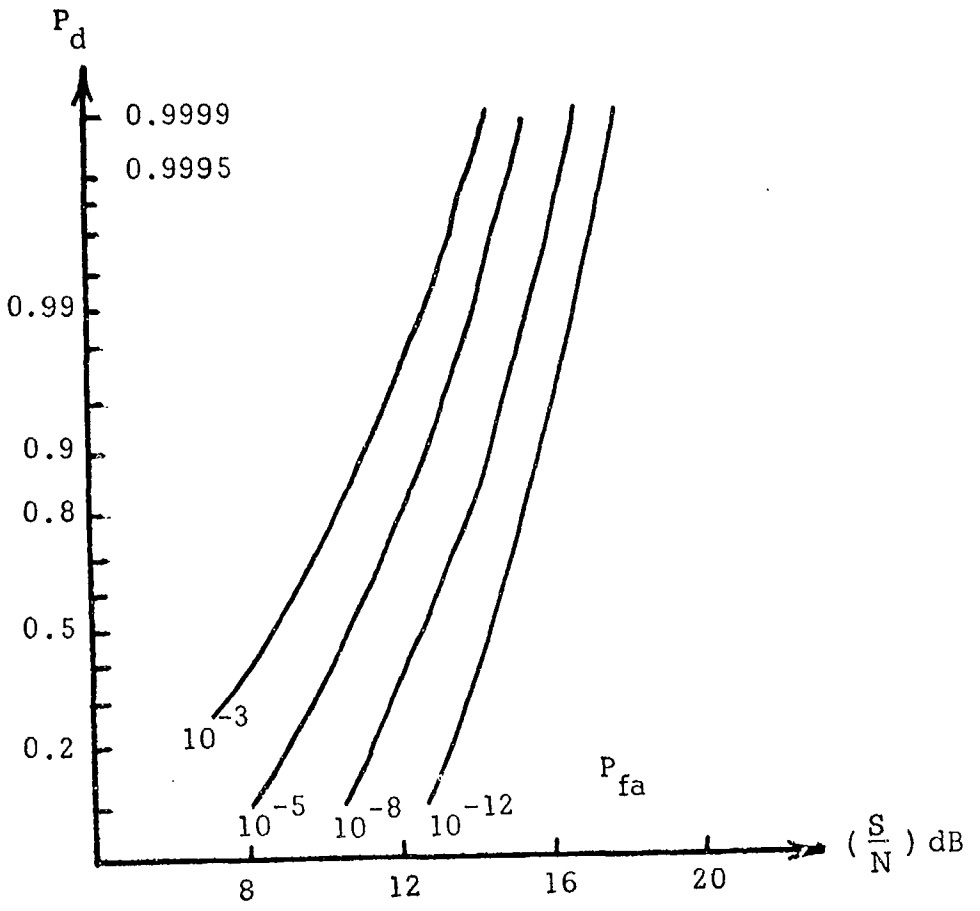

Figure 5. P_d Versus S/N and P_{fa}

where E is the signal energy, N_o is the noise power/Hz, B the bandwidth in Hz, and τ is the pulse width.

One will note that the results obtained are valid for the case where the signal received has exactly known characteristics, except for time of arrival, i.e., the radar receiver situation. The uncertainty generated by having to look for signal pulses of unknown frequency in a bandwidth W can be shown to significantly reduce the detectability index, d, where d becomes

$$d = \left(\frac{1}{4M}\right)\left(\frac{S}{N}\, 2B\tau\right)^2 \tag{12}$$

M is the number of signals possible in bandwidth W equal to the minimum duration of a given signal times the bandwidth, $W\tau_{min}$. It is apparent from equation (12) that this represents a considerable degredation of performance and is the cost of having to cover a broad frequency spectrum.

One can observe from Figure 5 that the design engineer will specify a detection probability and a false alarm rate. This will set V_t and automatically determine S/N minimum and the maximum range from target emitter. If one obtains a greater S/N than the minimum the figure clearly shows that with V_t set, P_{fa} is set and P_d increases. The key to a design that virtually eliminates P_d from receiver limitation studies is to set V_t for a specified P_{fa} and then demand or assume a $(S/N)_{min}$ greater than that S/N that would yield a P_d greater than 0.9999. In this way P_d will approach unity, noise is virtually eliminated as a factor in the successful intercept of a signal, and the limiting factors are reduced to scanning in frequency or space. If one requires P_d to approach unity,

one loses only 3-4 dB in sensitivity compared to accepting P_d much less than unity. One can show this result by working a few examples from Figure 6.

6. Noise Calculations in Representative Receivers

a. General

Once P_d and P_{fa} are determined, the design S/N requirement is set. Using this S/N the designer works backward through a realizable system to determine required input S/N. Receiver bandwidth, detector noise, and preamplifier gain, work to set receiver noise characteristics. Inadequate attention to proper design procedures at this point will negate careful calculations made prior to this stage in the design. This section will examine the effects of bandwidth, detectors, and gain in a superheterodyne and wide-band receiver. The evaluation will be made with the goal to optimize receiver performance, and illustrate factors that contribute to receiver noise characteristics.

b. Superheterodyne Receiver

Many modern superheterodyne receivers utilize digitally controlled tuning to facilitate interface with a digital processor. The General Instrument DCR-30 is typical of this type receiver. Figure 6 illustrates important digitally tuned superheterodyne features in block diagram form, and Figure 7, the noise and gain factors associated with the receiver.

Typical of this type receiver are suboctave filters in the rf preselector that are switched, not tracked, to the local oscillator.

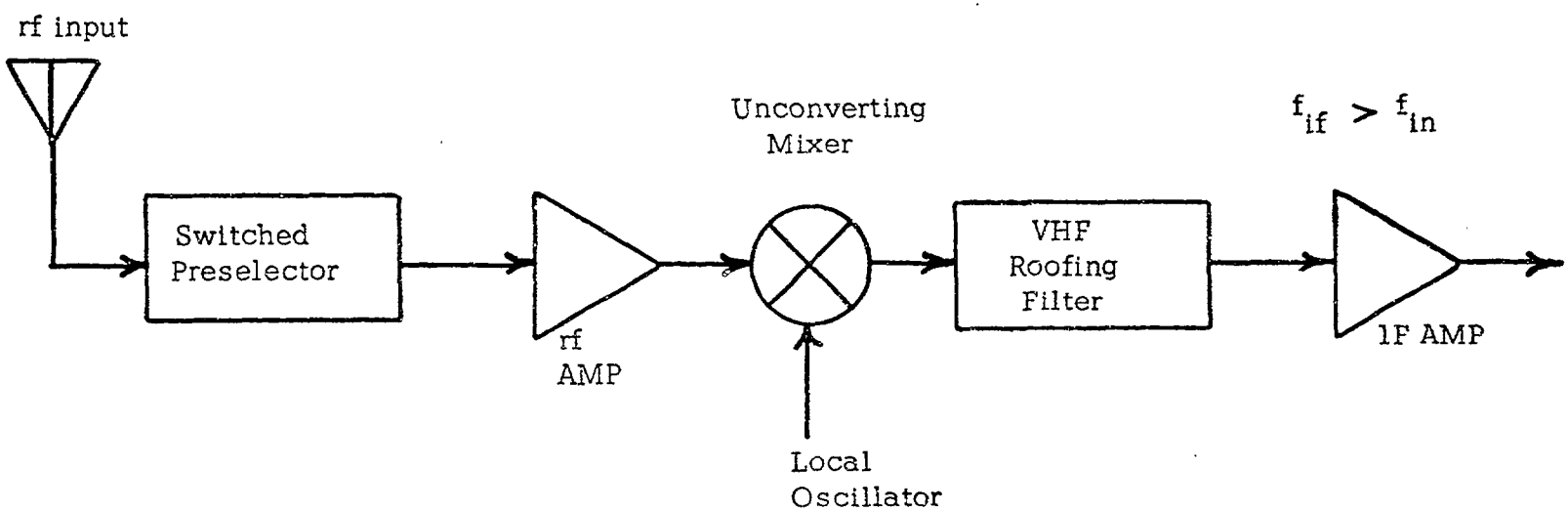

Figure 6. Digitally Controlled Superheterodyne Receiver

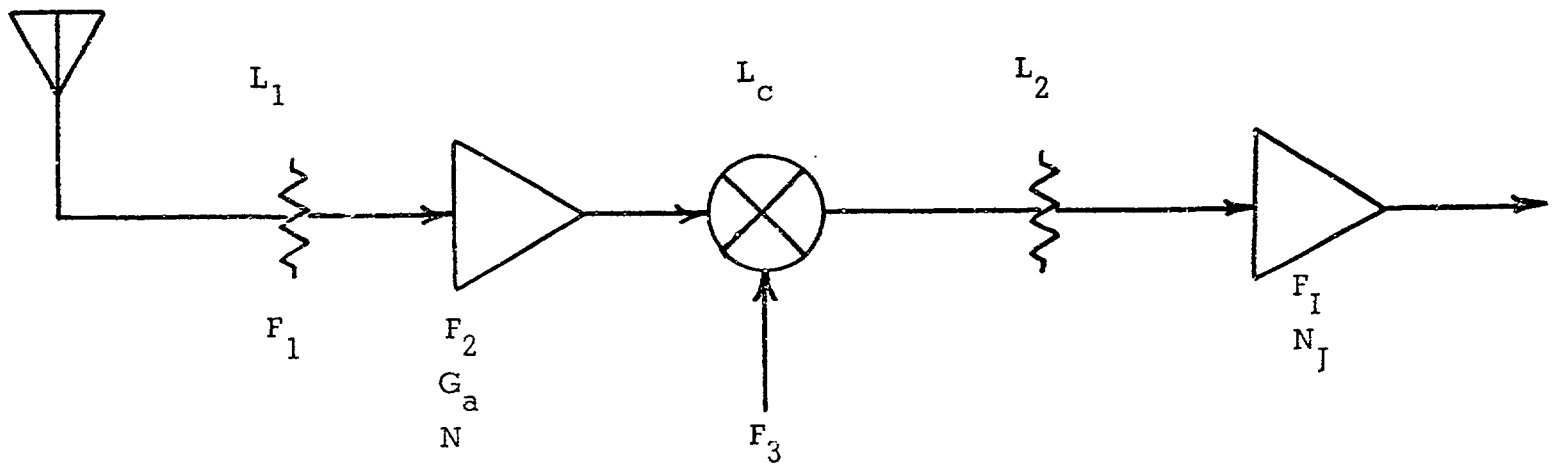

Figure 7. Noise and Gain Factors for Figure 16

To improve spurious response the incoming frequency is upconverted. Downconversion receivers are more apt to generate spurious responses in the mixing process that will fall within the rf amplifier pass band. The object of design is to maintain a maximum receiver dynamic range while minimizing noise figure. The use of suboctave switched filters degrade receiver performance by generating excess intermodulation distortion (IMD). [21] The design engineer must then minimize IMD generated elsewhere in the system in order to achieve a satisfactory noise figure. To avoid generating IMD in the rf amplifier one requires an rf gain well below saturation but high enough to confine noise (confining gain) to the input stage. These two requirements are obviously in conflict.

Appendix E demonstrates methods used to calculate superhet system noise figure using the concept of confining gain. It can be demonstrated that when the rf preamplifier gain is sufficiently high the system noise figure is reduced to the noise figure of the rf preamplifier. Such a system will have the lowest possible noise figure achievable with the particular preamplifier used. Further noise reduction methods are the use of low noise preamplifiers or cryogenic cooling of the existing amplifier. The noise figure of the preamplifier and external sources not under the designers control are the sources of interference the signal must work against and thus are the basic limitations to achieving high probability of detection in low signal strength situations.

When wide band components are used, their effects must be included in noise calculations. Consider Figure 8. In this configuration the YIG preselector filter is tracked with the local oscillator

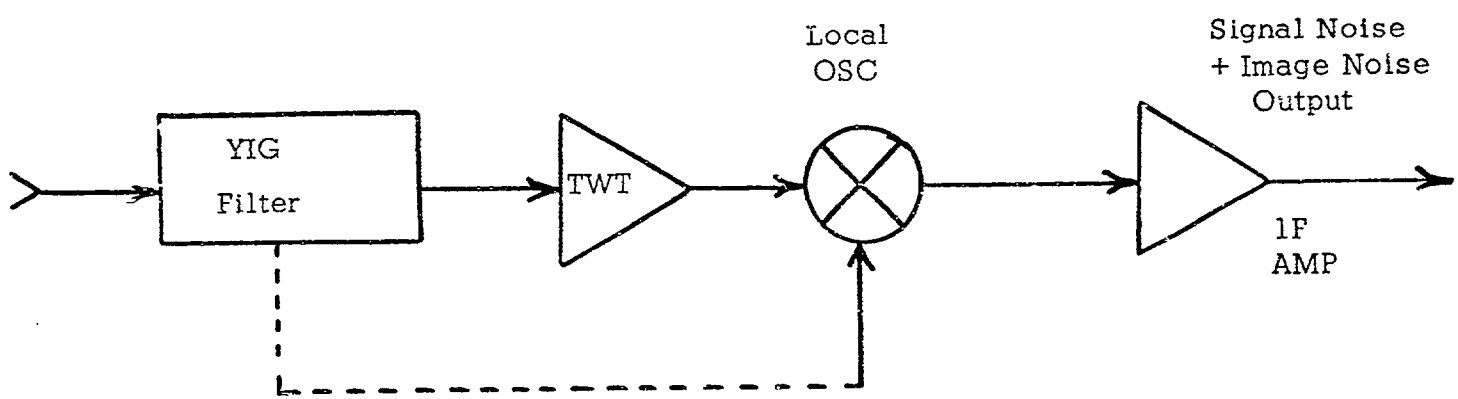

Figure 8. Superheterodyne Receiver with YIG Preselector

to reduce image and spurious responses to reduce the effect of strong out-of-band signals on the TWT. This system does not yield the lowest system sensitivity possible since the YIG filter losses must be added to the TWT noise figure. Excellent spurious rejection is obtained however. If the TWT bandwidth includes the image frequency the system will display a double-sideband noise figure 3 dB greater than the single-sideband noise figure. [21]

By placing the YIG filter after the TWT, Figure 9, the TWT gain confines the noise to the TWT noise figure (equation (E-8)), while filtering the image and allowing only a single-sideband of noise into the system. It is obvious however, that this system does not reduce IMD generated by strong out-of-band signals. In order to achieve the best of both worlds one could use two filters tracked in unison, one before the TWT and one after.

When the designer selects wide-band amplifiers he must be aware of the methods used by the vendor to test noise figure. Failure to do so could result in the designer assuming that the amplifier is 3 dB better than it really is if double-sideband noise will be present.

It may seem odd to the reader that bandwidth is not mentioned in this discussion. With the receivers discussed the rf pre-selector or YIG filter limits noise to a very narrow bandpass. Further, in Appendix B noise figure was related to bandwidth through equations (B-10) and (B-11). By specifying the noise figure one effectively specifies bandwidth, or equivalently, noise temperature.

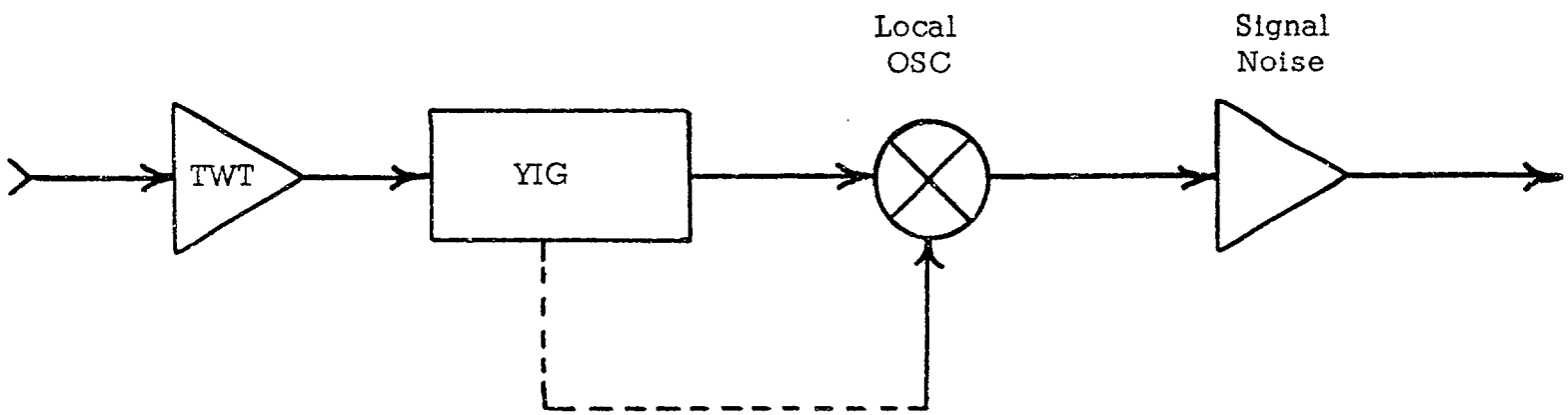

Figure 9. Superheterodyne Receiver YIG after TWT

c. Wideband Receivers

When the probability of intercept needs to be maximized, wideband receivers are a natural choice. Assuming that signal is greater than noise by an amount sufficient to reduce P_{fa} to an acceptable level and provide processing equipment with "clean" information, probability of intercept in a wideband system is unity for signals in-band. Wideband receivers are popular in threat-warning systems where probability of intercept must approach unity and the cost must be kept low in production numbers. Consider Figure 10.

Figure 10 indicates a simple wideband crystal video receiver. In typical systems octave rf bandpass with video bandpass sufficient to preserve pulse rise time are found. With many radar systems using very narrow pulse widths a video bandpass of 10 MHz is not uncommon. [21]

The difficulty encountered in calculating sensitivity in wideband systems is that the rf allows noise of bandwidth B_{rf} to enter the system while the video will accept noise of bandwidth B_v. One must calculate an effective bandwidth that conveniently describes the actual system response to these two distinctly different bandwidths. Ayer [22] developed a method of calculation that determines the effective bandwidth, B_e, for systems using square-law detectors to be

$$B_e \simeq \sqrt{2 B_v B_{rf} - B_v^2} \tag{14}$$

This is a commonly used equation utilized to calculate system sensitivity. Equation (14) is found to be a good approximation when B_{rf} is much greater

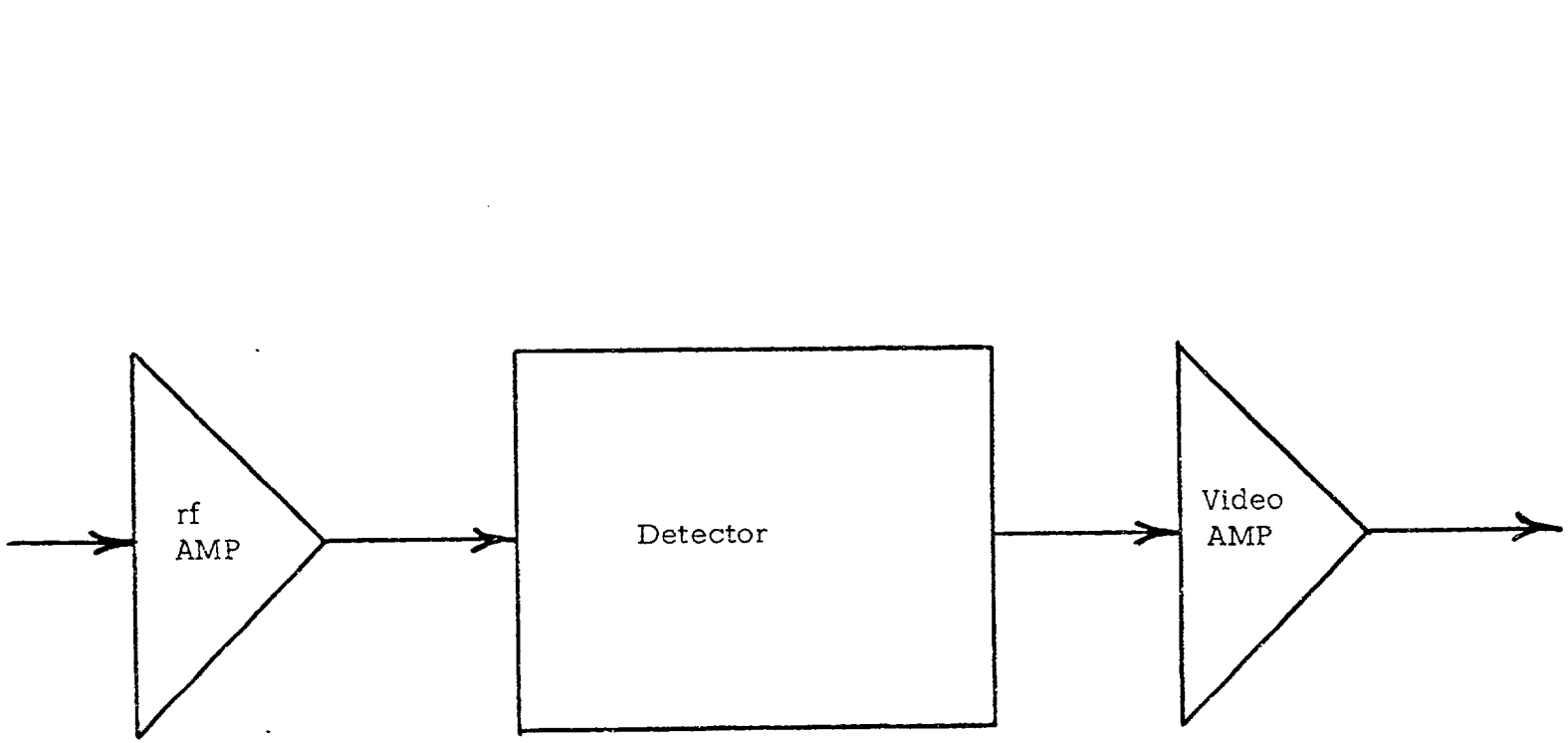

Figure 10. Wide Band Crystal Video Receiver

than B_v. Klipper [23] related the video bandwidth and rf bandwidth to both linear and square-law detectors by developing equations relating input S/N to output S/N for various sensitivity definitions.

There are three sensitivity definitions in common usage, minimum discernible signal (MDS), signal equal to twice noise, and tangential sensitivity. Minimum discernible signal is defined for a CW signal as the input signal that will produce a total output power twice the value of the power output with noise input only. This is not $S_o/N_o = 1$ since the output noise is a function of mixing products with the signal which increases noise output in the presence of a signal. Signal equal to twice noise is defined for a CW signal as the input that will produce output signal power equal to twice the value of the noise power alone. Tangential sensitivity is defined for a pulse signal as that input signal level that will result in an output where the top of the noise along the base line is at the same level as the bottom of the noise on the pulse as illustrated in Figure 11.

Klipper through a detailed analysis demonstrated for both linear and square-law detectors

$$\frac{S_o}{N_o} = \frac{(S_i/N_i)^2}{a + b(S_i/N_i)} \tag{15}$$

where a and b are constants related to the rf and video bandwidths. It can be demonstrated that the tangential sensitivity for a system using a square-law detector is

$$\text{Tang Sens} = KT_o F\left(7\sqrt{2B_{rf}B_v - B_v^2} + 49\,B_v\right) \tag{16}$$

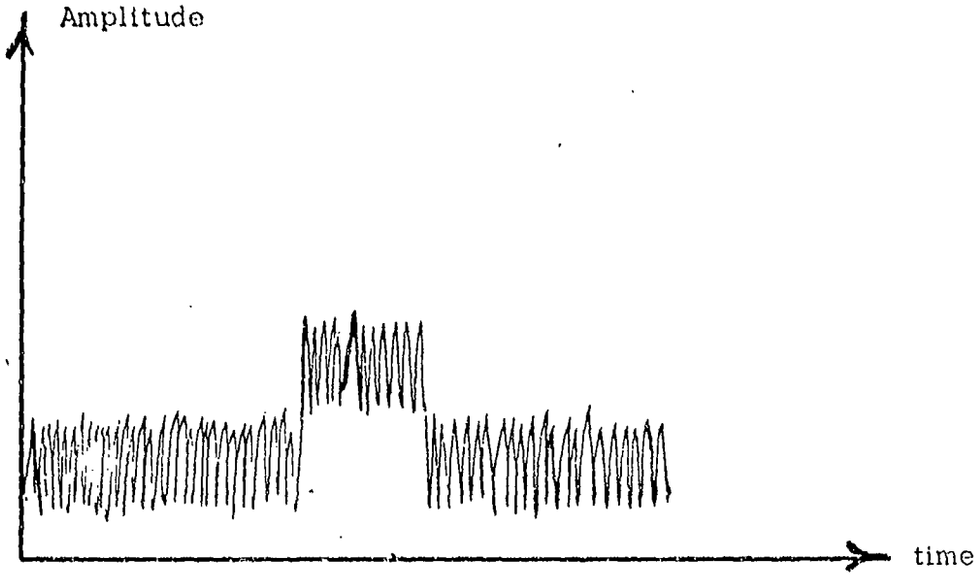

Figure 11. Tangential Sensitivity

where F is the system noise figure, approximately equal to the noise figure of the rf amplifier so long as the rf gain is large, confining the system noise to the rf amplifier noise figure. The reader will recognize the quantity under the radical to be the Ayer formula for effective bandwidth. When B_{rf} is much greater than B_v equation (16) reduces to

$$\text{Tang Sens} = K T_o F \sqrt{2 B_{rf} B_v} \tag{17}$$

Klipper defines effective bandwidth for a system with a square-law detector as

$$B_e = \sqrt{2 B_{rf} B_v} \tag{18}$$

Note that the Ayer formula reduces to exactly the same quantity when $B_{rf} \gg B_v$. If one assumes $B_{rf} \gg B_v$, sensitivity can be written as

$$\text{Sens}_{dbm} = -114 + F_{dB} + D_{dB} + 10 \log_{10}(2 B_{rf} B_v) \tag{19}$$

where -114 is $10 \log k T_o$ in dBm, $T_o = 290°K$, and D is a function of the type of detector and sensitivity definition used. Figure 12 is a plot of equation (19) for various video bandwidths. Table I lists values of D to be used with Figure 12.

	MDS	$S_o/N_o = 1$	$S_o/N_o = 2$	Tangential
Square-law	0	0	1.5	8.5
Linear	-3	-3	-1.5	5.5

TABLE I. VALUES OF D TO BE USED WITH FIGURE 12

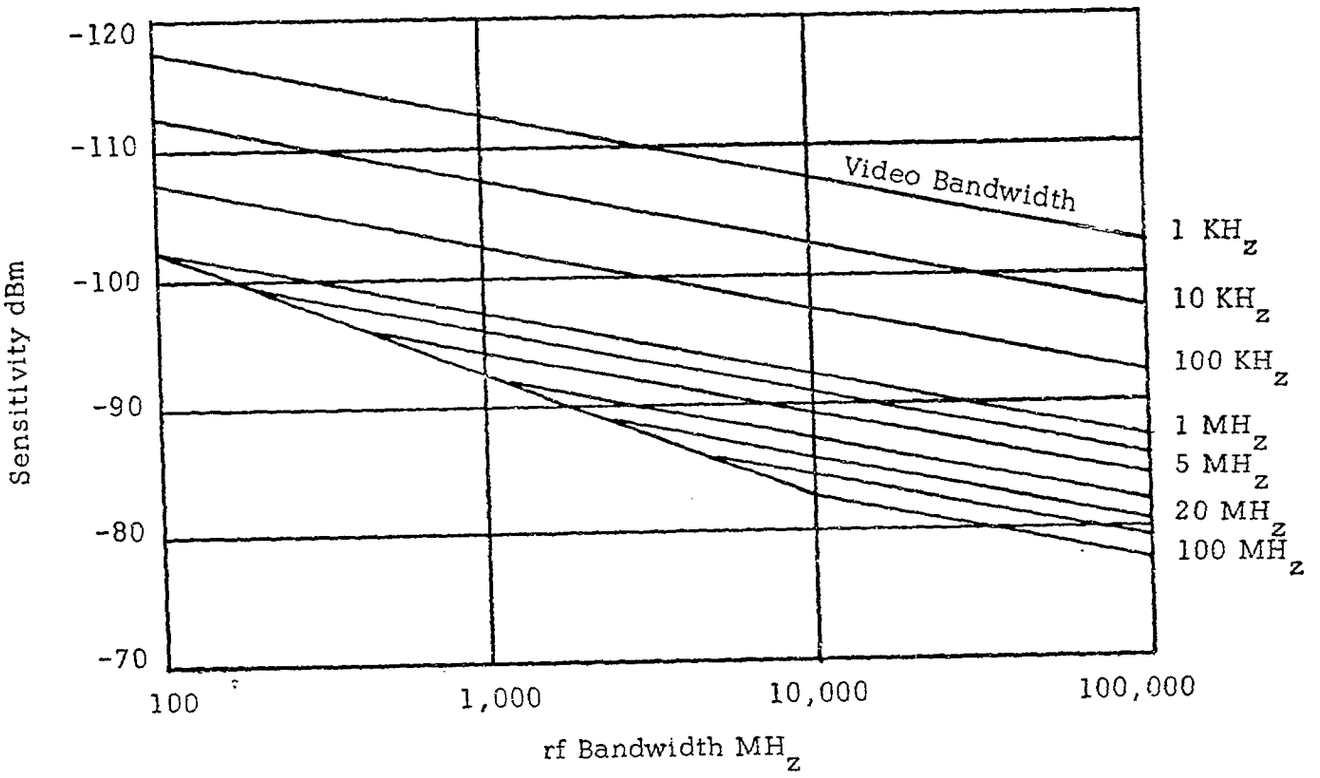

Figure 12. Sensitivity Versus Bandwidth, Wide Band System

B. SCANNING FACTORS

1. General

Multiple channel receivers such as likelihood ratio receivers and the AN/SLQ-12 two-tuple receiver are complex and expensive. Therefore, scanning and wide-open receivers are utilized almost exclusively in today's intercept systems. However, technological advances in miniaturization and component integration are leading to a re-examination of the potential replacement of crystal video, IFM, and scanning receivers with multichannel channelized receivers. [3] Intercept receivers fall into two basic categories; the wideband system and the scanning or panoramic superheterodyne type. In addition to frequency scan one must consider the effects of transmitting antenna scan if one utilizes a directional antenna for either direction finding or high gain for added sensitivity. In both the frequency scan and spatial scan cases the problem is to determine when the receiver and transmitter are coincident so that an intercept may be accomplished. The problem of determining coincidence is the so called scan-on-scan problem. Richards [4] reduced the problem of calculating the probability of coincidence of two regular scanning systems to the problem of calculating the probability of coincidence between two regular pulse trains. Figure 13 illustrates the pulse-train situation for a rotating receiving antenna and rotating transmitting antenna, while Figure 14 illustrates the temporal problem of transmitter duty cycle and receiver scan characteristics.

For Figure 13 define

T_{ta} = transmitting antenna rotation period

t_{ta} = transmitting antenna look period = B_t $BW_{ta}/360°$

BWta = beamwidth of transmitting antenna

For Figure 14 define

PRI = pulse rate interval

PW = pulse width

Ts = receiver scan time (time to scan frequency spectrum)

Ta = receiver acceptance time

The receiver acceptance time is a function of the receiver acceptance bandwidth, Ba, the time required to cover the total frequency bandwidth Ts, and the spectrum covered by the signal. The Fourier transform for pulsed signals yields a $(\frac{\text{SIN } x}{x})^2$ power spectral density with approximately 90% of the signal energy contained in a bandwidth of PW^{-1}. Since the signal would just be detected if the acceptance bandwidth were on the outer edge of the signal power spectral distribution the receiver acceptance time is defined by

$$Ta = \frac{PW^{-1} + Ba}{S} \tag{20}$$

where S is the receiver sweep rate. One may determine the probability of coincidence of either set of pulse trains by one of two methods. The first, graphically, is quite straight-forward and can be accomplished with little rigor. The second is to refer to the analysis by Richards [4] and to determine the probability of coincidence mathematically. Richards'

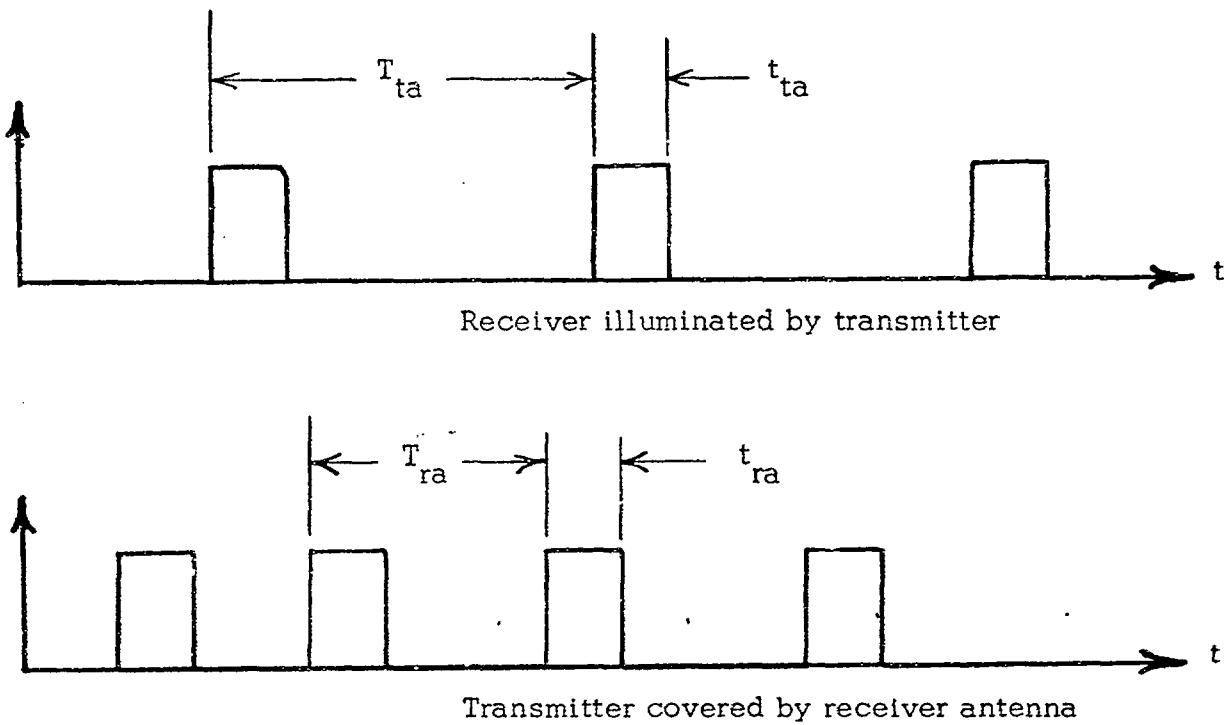

Figure 13. Antenna Scan Pulse Train

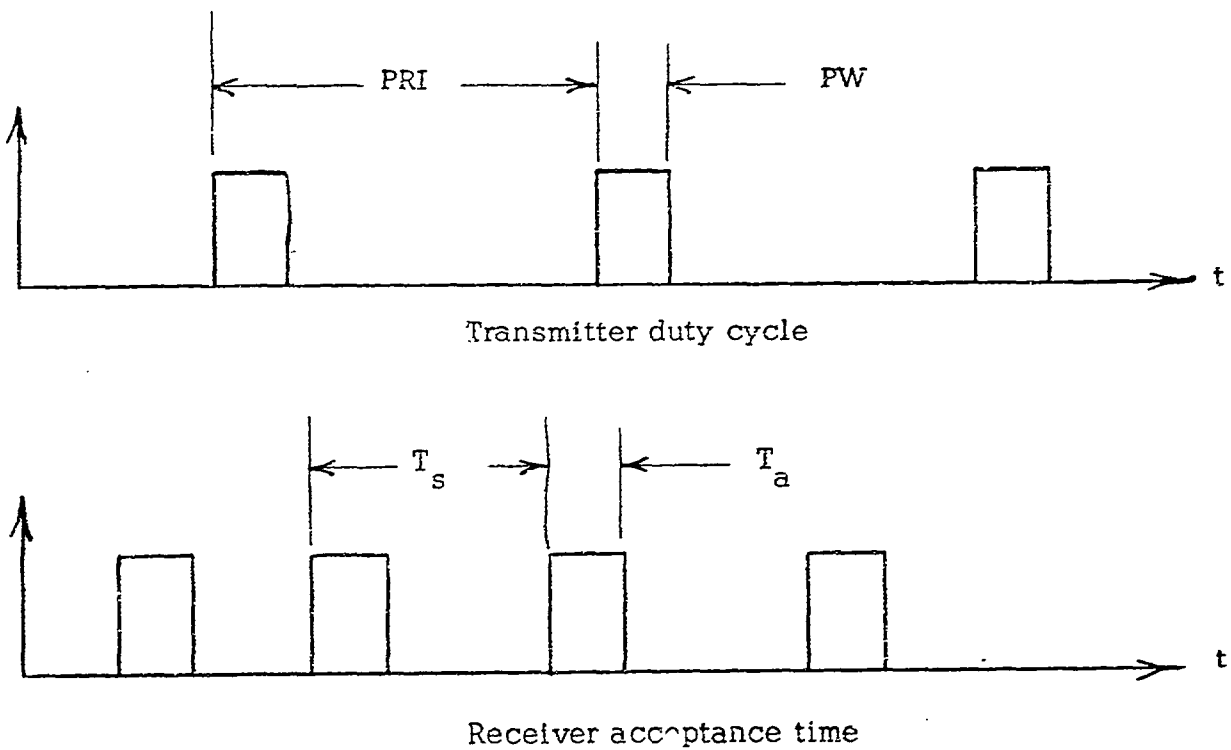

Figure 14. Frequency Scan Pulse Train

method will be demonstrated in a later section. An alternative graphical analysis is the frequency time graph illustrated in Figure 15.

Define:

Fl = lower rf limit

Fu = upper rf limit

Fs = signal frequency

The advantage of using the frequency-time graph is that the problem of extending the graph to obtain coincidence reduces to preparing periodic parallel lines; making the method faster than the pulse train method described above.

2. Probability of Intercepting a Signal in One Receiver Scan

Referring to Figure 15 one can observe that if the pulse repetition interval is greater than receiver scan time at most only a single pulse can occur in one scan period. The probability that the single pulse will coincide with the receiver acceptance bandwidth may be calculated as the ratio of pulse width plus receiver acceptance time, equation (20), to the receiver scan time

$$POI[1] = \frac{PW + Ta}{Ts} \tag{21}$$

where POI [1] is the probability of intercept on a single sweep. When the pulse repetition interval is less than the receiver scan time more than one pulse occurs in one receiver scan time. The number of pulses that will occur can be determined by comparing the pulse rate interval to the scan rate. For example, if the receiver scans at 10 sweeps per second

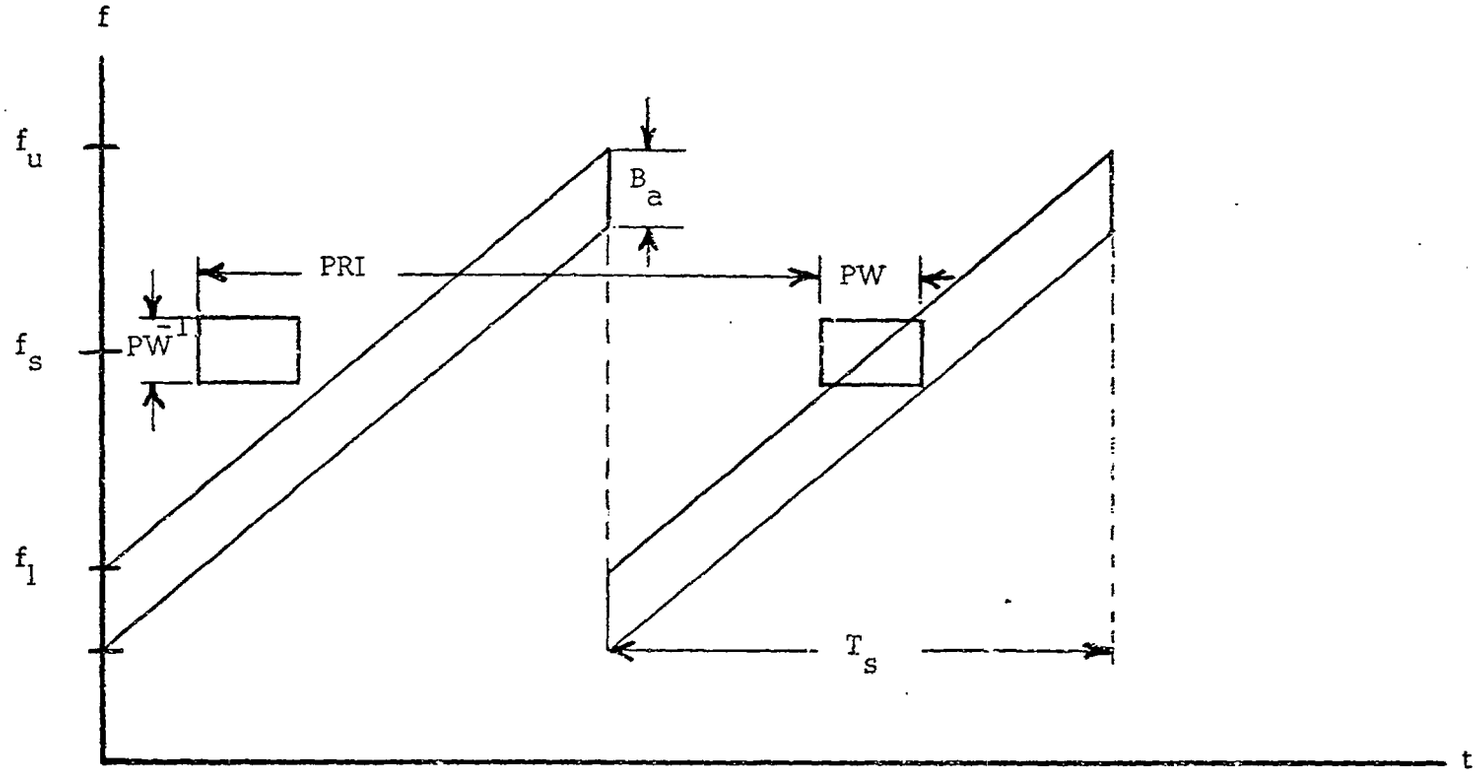

Figure 15. Frequency Time Graph

(0.1 second per sweep) and the signal contains 1000 pulses per second, the number of pulses in one scan is simply (0.1 $\frac{\text{sec.}}{\text{sweep}}$) (1000 $\frac{\text{pulses}}{\text{sec}}$) = 100 $\frac{\text{pulses}}{\text{sweep}}$ or

$$N_p = (T_s)\,PRF \tag{22}$$

where N_p = number of pulses in a single sweep. From probability theory [16] the probability of a coincidence is now N_p greater than the probability of coincidence for a single pulse.

$$POI_s = N_p \left[\frac{PW + Ta}{T_s} \right] \tag{23}$$

Since $N_p = \frac{Ts}{Tp}$, where $Tp = PRF^{-1}$, the equation is valid until Tp = PW + Ta when equation (23) reduces to

$$POI_s = \frac{T_s}{T_p} \left[\frac{PW + Ta}{T_s} \right] = 1 \tag{24}$$

As long as Tp $<$ PW + Ta equation (23) is unity and at least one coincidence is assured.

The discussion to this point has considered frequency scan only. The same principles apply in determining antenna scan coincidence.

One factor ignored to this point is the complication introduced by the possibility of synchronization of the scan rates of the receiver and transmitter in angle. If one supposes a receiving antenna system covering 360° the antenna scan problem reduces to a consideration of the fraction of time the transmitting antenna illuminates the receiving antenna

$$POI_a = \frac{t_{ta}}{T_{ta}} \tag{25}$$

where POI_a is the probability of intercepting based on the antenna scan characteristic. For statistically independent events the probability of both events occurring simultaneously is the product of the individual probabilities. The overall probability of intercept in a single frequency scan is given by

$$POI = POI_a (POI_s) = \left(\frac{t_{ta}}{T_{ta}}\right)\left(N_p \frac{PW + T_a}{T_s}\right) \tag{26}$$

The single most important result of the analysis above is that one can show that if the probability of coincidence on one scan is less than unity, the time required to achieve a specific intercept probability is inversely proportional to the probability of intercept per scan. [1] It is apparent that this is the price one must pay to go from a wide-open omnidirectional system to a superheterodyne panoramic receiver with a scanning antenna. To reduce search time one must either increase the probability of intercept or scan in frequency at increased rate. The Operational Evaluation Group, Office of the Chief of Naval Operations, in OEG Study 294 [24] demonstrated that for an intercept system scanning both frequency and azimuth, one scan should be done slowly while the other should be done as rapidly as possible. Where only one type of scan is used, the scan rate should be done as rapidly as feasible. A greatly simplified discussion of the effects of receiver scan characteristic may be found in Schlesinger, et. al. [25]

3. Intercept Receiver Scan Rates

Frequency scanning intercept receivers may be divided into three categories depending on speed of scan. Slow-scan receivers include those manually-tuned by an operator and those automatically scanned across the rf bandwidth in the time of several transmitter antenna scan periods. Receivers of this type typically possess times to achieve intercept measured in minutes. Typical of this type are certain obsolete shipboard intercept receivers. In modern warfare where weapon systems are able to begin radiating, detect targets, launch weapons, and shut down in a matter of seconds, the slow scan receiver is unacceptable.

Intermediate scan receivers are those that complete one frequency scan in one transmitter scan period or less. In this region it is likely that a synchronization will occur between scan rates at either the transmitter scan period or exact fraction thereof. Similar to the slow scan case, the time to intercept is unacceptably long, rendering such a system equally unacceptable.

Rapid-scan receivers comprise the majority of modern efficient intercept receivers. Three rapid-scan type receivers exist. Those with an rf scan comparable to the duration of a radar look are quite common. If one considers the case where the scan period of the intercepted signal is equal to the rf scan period, it is obvious that some pulses will be detected every scan.

The number of pulses received during each receiver scan period is the pulse-repetition frequency of a radar times the total time

the receiver spends on the transmitted frequency

$$\text{Pulses intercepted} = (PRF)\frac{B_a}{B}\ T_s \tag{27}$$

where B is the rf bandwidth.

The maximum time to intercept with the system outlined above is the receiver scan period Ts. One notes that equation (27) is valid so long as the receiver sweep interval is greater than the pulse rate interval. Otherwise it is possible that the acceptance bandwidth may exist only between radar pulses. The minimum receiver scan period is given by

$$T_{s(MIN)} = \frac{B}{B_a}\ PRI \tag{28}$$

One can verify equation (28) by constructing a frequency-time graph similar to Figure 15 for PRI and scan period and by varying scan period for a fixed PRI. Typical of this type receiver are the Watkins-Johnson WJ-940 [26] and WJ-1007 receivers. The WJ-1007 microwave collection system has a digital scan rate variable from $0.3GH_z$ to $300GH_z$ per second over an $18GH_z$ bandwidth. [27] The upper rate corresponds to a receiver acceptance time of 0.06 sec. or to a narrow beamwidth rapidly scanning radar.

Receivers with an rf scanning rate comparable to the transmitter pulse repetition frequency follow an analysis similar to that above. In a single receiver scan period the receiver will intercept at most a single pulse from each signal present. In searching for continuous pulsed emitters, the digitally tuned superheterodyne receiver, whatever its acceptance bandwidth, waits at each rf window for a time equal to or

exceeding the maximum PRI expected. A receiver configured in this manner will possess a probability of intercept of unity for signals whose PRI is less than the wait time at each rf window. [28]

Receiver scan periods comparable to pulse-width are known as micro-scan receivers. By scanning the rf passband in one pulse width, the POI for a single pulse is unity provided signal strength is sufficient. The ability to measure pulse width and pulse repetition frequency is degraded due to the "chopping" effect of the receiver scan. Due to the chopping effect the input pulse is divided into segments less than a pulse width wide. To preserve the integrity of the pulsed information the system then requires a wider video bandwidth than previous systems. In addition, the amount of energy available for display and processing is limited. Recent work in the field has sought to overcome these difficulties. Typical of modern microscan receivers is the Stanford Research Institute SR 1965-A Microscan Receiver. The SR-1965-A scans in frequency every 0.667 sec., which provides a POI = 1 for pulses larger than the scan time. A high probability of intercept is achieved for pulses of shorter duration. Pulse compression techniques in the i-f stage result in the receiver achieving a sensitivity of -100 dbm in the 2-4 GH_z band with a frequency resolution of 4.8 MH_z. The pulse compression obtained in the video results in the signal power leaving the compression filter in a "compressed" pulse whose width is a function of the i-f band pass with pulse duration approximately equal to the reciprocal of the i-f bandwidth. Not only does the technique result in an increased frequency resolution but the narrowed pulse corresponds to a higher peak power overcoming the limitation of low power.

C. MODULATION FACTORS

In addition to scanning in azimuth and frequency the receiver must be able to demodulate the signal to complete a successful signal intercept. Radar signals may have many types of modulation including constant wave (CW), pulsed, and pulsed FM or "chirp" radars. In addition to interpulse modulation the radar may transmit on more than one frequency simultaneously (multi-beam), or may be frequency agile--hopping or sweeping over a specific frequency range either periodically or randomly. To provide effective countermeasures or to correctly identify and classify radar types, it is necessary that the system detect the various types of modulation contained in radar signals. In many cases, modulation recovery may be accomplished by recording pre-detected signals and performing detailed signal analysis off-line and post-mission. Where time is of the essence, it is necessary that signals be sorted and classified so that real-time and on-line countermeasures may be applied. Failure to properly detect modulation can then be considered as a degradation to system probability of intercept since by definition the system fails to accomplish its mission.

Many receivers are configured with multiple, parallel detector types (i.e., discriminator for pulsed FM, square-law detector for pulsed signals) so that various modulations can be detected by noting the detector where signal output is greatest.

A superheterodyne receiver's ability to detect signals is limited by the scan characteristics of the receiver and interference between signals close in frequency. The ability of a superheterodyne to recognize a

frequency agile radar is severely limited. A frequency hopping or sweeping radar will appear as multiple emitters to the receiver. Chirp radars where the frequency deviation is greater than the acceptance bandwidth will not be detected correctly. Depending on the receiver and chirp radar frequency scan rates the signal may appear as multiple emitters, or as a signal spread over a very wide frequency spectrum, or as a combination of the two on succeeding receiver scans. Obviously this condition degrades the ability of an automatic system to classify the signal properly and will result in a degraded POI since time to intercept is increased. CW signals appear as pulsed radars with a pulse width equal to the receiver acceptance time. Pulse radars will appear normally except for a pulse width modulation imposed by the acceptance bandwidth. By providing a separate manual tuned analysis receiver the degradation to analysis on CW signals, pulsed signals and chirp signals is minimal. However, the manual tuned receiver will still be unable to analyze the frequency agile radar unless the acceptance bandwidth is wider than the total frequency excursion.

Multiple signals arriving within the receiver acceptance bandwidth will generate ambiguous signals due to mixing products generated in the detector stage. The probability that multiple signals occur within the narrow passband in a superheterodyne is extremely low however and normally will not adversely affect system POI.

Wideband systems are affected in a much different manner. Chirp radars, frequency agile radars and pulsed radars will enter the RF section and provided the proper demodulator is provided, signals will be detected.

However, a frequency agile radar will appear as a normal pulsed radar since all frequency information is lost. A CW signal will be detected normally as will pulsed signals. Since FM information is not destroyed by the wideband system, it may recover the chirp signal through an FM demodulator. The wideband system is able to alarm the presence of all signals in-band but is not able to identify frequency agile or multi-frequency radars operating in PRF synchronization. Simultaneous signals in the wideband system will generate mixing products in the detector stage. The mixing products adversely affect computer based recognition systems when simultaneous signal duration is excessive causing increased input data rates. This excessive duration can occur with multi-frequency radars used for weapons directing systems. For radar warning system applications, the simultaneous arrival of signals does not degrade performance since the human ear will not detect microsecond overlaps but responds to signal components over a much longer time period.

D. RECEIVING ANTENNAS

Three factors affect the choice of antennas related to POI in an ECM system; gain, direction finding, and polarization. A requirement for high gain antennas limits choice to either parabolic, horn, or phased array antennas, all highly directional. The directional features result in a severely decreased intercept probability when both the receiver and antenna must scan. By using non-scanning receivers such as IFM's or wide-open crystal-video receivers one obtains a sensitivity greater than

with omni antennas and reduces the scan problem to that of spatial scan. [30] The methods used to calculate POI in previous sections then apply.

Direction finding requirements lead to several different antenna systems. Simplest is the rotating highly directional horn or parabolic type antenna. The degredation to POI as a result of a choice of this system was covered above. An alternative method would be to utilize more than one antenna to obtain DF by either measuring time of arrival (TOA) or direction of arrival (DOA). Two antennas result in an ambiguity in direction. Therefore, as a minimum, three or more antennas are utilized to provide an unambiguous DF capability. Quadrature spiral antennas are used to provide DF with significant accuracy in an Applied Technology System for the U. S. Navy's EA-6B Electronic Warfare Aircraft. [28] General Instrument Corporation's POINTER radar warning receiver utilizes a similar quadrature spiral arrangement for DF. [31] The advantage of using quadrature antennas is that the non-scanning antenna maintains the intercept capability of an omnidirectional antenna. Various other methods for direction finding may be found in Harris, et. al., chapter 10, Ref. 1. Application of the IFM type receiver with various antenna systems will be covered in detail in a later section.

Antenna polarization requirements arise due to the nature of signals in an ECM environment. A maneuvering intercept platform or maneuvering transmitting target may cause signals of various polarizations to arrive at the receiver. In the short time periods allowed for intercept one cannot afford the luxury in either time or expense to provide multiple antennas

with different polarization. It is necessary, therefore, to use circularly polarized antennas that meet the system requirements of gain, bandwidth and beamwidth, while enabling the system to respond to any orientation of linearly polarized threat signals. Failure to provide antennas with the polarization required will reduce probability of intercept considerably. Commonly used ECM antennas that meet the requirements listed are spirals and horns. Horn antennas are basically linearly polarized. Circular polarization is achieved by a variety of methods, including using quadrature hybrids, a layered polarizer, or by twisting the throat 45°. Horns are capable of gains up to 20 dB and of handling large power levels. Horns have narrower beamwidth, lower bandwidth (octave), higher weight and cost than spirals.

Spiral antennas are naturally circularly polarized. A major advantage over horns is the spirals' extremely wide bandwidth possible through careful design, (approximately 10:1, greater than 3 octaves). Spirals have a larger beamwidth (up to 90°), are lower in weight and cost, handle less power, and have a lower gain than horns. An advantage of horn type antennas are their ability to be more easily bent and squeezed into available space. [32]

E. SIGNAL PROCESSORS AND SIGNAL DENSITY

In automated intercept systems such as those found in warning receivers, deception receivers, and some general purpose intercept receivers, the probability of intercept depends on the processing peripherals in addition to the basic POI of the receiver. Unless the computer

absorbs input data as it is received and transmits the output data to other devices as fast as they require, the computer will degrade the system. [38] The trend toward computer-controlled intercept systems is seen by many as a logical step. Considering the complexity and variety of weapons systems now appearing, a major drawback to computer controlled systems is a lack of adaptability and versatility. Electronic Warfare computers like the ITEK ATAC-8 and General Instrument's POINTER computer aim to provide some versatility by providing programmable signal recognition files.

The EW community is leaning heavily on wide-band systems with POI approaching unity. Considering today's dense ECM environment high data rates close to and exceeding the capability of a typical minicomputer may be expected. Parallel processing and pre-analysis sorting techniques will allow data levels compatible with computer speeds. [3]

Digital processing requires "clean pulses" in order to perform without excessive error. The requirement for "clean" pulses implies a need for increased S/N ratio. The need for increased S/N means the system must either provide additional sensitivity through antennas or preamplification, or shorten intercept ranges. In either case it is obvious that the probability of intercept for a particular system is degraded because of the requirement for increased S/N. [21,28] The point made above is a subtle one since the user generally does not consider a system operated in accordance with design as degraded. However, without the S/N required by a computer,

more reliable interception is made on close signals, and signals at long range may be intercepted that otherwise may have been missed.

The algorithms used to sort signals and determine signal characteristics directly affect POI. Depending on the processor, various numbers of pulses are required to successfully identify a signal. In most computer controlled systems more than a single pulse is necessary in order for the sorting algorithm to identify the signal. Scan analysis, for example, typically require in excess of 50 pulses. ITEK's ATAC-8 builds a pulse amplitude histogram to analyze scan. The histogram effectively averages missed pulses over many pulses to generate I.D. keyed to scan type or rate. If for some reason the system cannot respond to enough pulses to determine I.D. the processor will drop the signal and fail to give an indication of signal to the operator. Where the user expects an alarm to indicate signals present, the failure to present the signal amounts to a probability of intercept of zero. Such an event could occur with scanning systems either in frequency or space where signal is intercepted but not for a time sufficient for the processor to complete its analysis, or it could occur when the input pulse density saturates the processor creating an overload situation. When all input storage bins fill, new information is lost or alternatively, the oldest stored information dumped. Either way, the process results in a degraded POI.

The problem of threat identification in a dense ECM environment is a matter of great concern to those in Electronic Warfare. [5] Current estimates of signal density predict 100,000 pulses per second per frequency band. [31] Intelligence estimates in 1959 expected 4000 important

signals/per second in the frequency range 500 - 12,000 MH_z, where an important signal is defined as a potential threat in a heavily defended area. 4,000 signals per second in a 5 band range corresponds to a pulse density of approximately 400,000 pulses/second. [1] Each signal pulse received must be accompanied by an internally generated processor word corresponding to time of arrival, direction of arrival (if DF equipped) frequency, and amplitude. One can readily observe that a large bit capacity is required if the system is to avoid overload and loss of data.

In a dense environment the two factors which have a major affect on the number of pulses missed are the received pulse widths and the A-D conversion rate of the system front end. Both effects work to create a period of time over which pulse analysis cannot be made. This time period is commonly known as "dead time". The A-D conversion is normally set by design. In cases where the A-D conversion rate is a limiting factor a brute force approach to decreasing "dead time" is to increase the A-D conversion rate. Since expense and complexity increase with A-D conversion rates, the point where cost factors outweigh A-D conversion speed is quickly reached. The overall effect of increasing conversion speed is to shift the high data rate to the interface between the A-D converter and processor. To handle this high data rate, digital buffering is required to prevent loss of data and hence degraded POI. Charge coupled device (CCD's) currently available are being applied in the development of buffering techniques to handle high data rates.

Processors and minicomputers operate at average data processing rates that ideally match the input data rate. Buffering techniques under development will allow the system to accept data at peak rates of arrival while processing at average rates. The effect is to smooth the data rate to an average rate of arrival. Through this method the designer is banking on the fact that very high data rates, corresponding to dense ECM environments, will occur for short bursts.

Pulse width generates a "dead time" in that amplitude and angle DF measurements will tend to be in error for other pulses arriving when a pulse is already present. Individual pulse time of arrival could still be measured. Simultaneous pulse arrivals generate additional difficulties to Instantaneous Frequency Monitoring receivers (IFM's). In dense ECM environments one would suspect that the problem outlined above could result in severe degradation to the intercept system. Therefore, one must examine the probability that simultaneous pulses occur. Hewitt [29] examined the simultaneous arrival question in the analysis of the microscan receiver. Assume that N independent emitters with duty cycle K are in the neighborhood of the receiver. The probability that two or more pulses arrive simultaneously is

$$P_t = 1 - (P_z + P_u) \tag{29}$$

Where Pz = Prob (no pulse present)

Pu = Prob (1 pulse present)

Let P_x be the probability that X pulses are present given by the binominal probability distribution.

$$P_x = \binom{N}{x} K^x (1-K)^{N-x} \tag{30}$$

Using equation (30) one obtains

$$P_z = \binom{N}{0} (1-K)^N \tag{31}$$

then P_t is given by

$$P_t = 1 - \binom{N}{0}(1-K)^N - NK(1-K)^{N-1} \tag{32}$$

Assuming 100 independent radars with a duty cycle of 0.001, $P_t = 0.005$. Against spatially scanning radars the probability of coincidence is decreased by the probability of two radars illuminating the receiving antenna simultaneously. Assuming a radar scan duty cycle of 0.005, the probability of a coincidence is 0.09. Since the two probabilities are independent, the overall probability of a coincidence is 0.005 X 0.09 or 4.5×10^{-4}. Where all radars are scanning the probability of a coincidence is very small. This analysis does not include multiple frequency fire control radars directed toward the intercept platform. Multiple frequency radars and multi-radar sites present the greatest problem in that it is a certainty that simultaneous signals will be directed toward the intercept platform.

The possibility of errors must be accounted for in the design of ECM computers. The data handling rate of the input must be sufficiently great to accept the normal signal data and not overload when overlapping pulses occur. When simultaneous pulses occur, signal sorting by measurement of angle and amplitude is degraded resulting in a complication of the sorting and analysis problem. One method used to overcome this loss is to reduce the probability of a simultaneous arrival. Frequency segmentation

is one method to reduce pulse density while angle sorting using sectored antennas is another. Channelization in frequency or direction results in increased cost. ITEK's preferred solution is to meet the data rate through the design of an EW computer capable of handling very high data rates without special purpose buffers. The ATAC-8 can simultaneously collect radar pulse train data from the antennas and transmit a different set of data to displays at high speeds. Parallel high speed processing permits tracking and de-interleaving of multiple pulse trains to be performed in high speed memory. [33] The Pointer system from General Instrument is similar in concept although operating at slightly slower data rates. [31]

With current large scale integration techniques in Programmable Read Only Memory (PROM), the designer is able to miniaturize hardware capable of generating pulse histograms. A histogram is generated by recording the number of pulses at a particular amplitude over a set observation time. The result is an amplitude probability distribution unique to the function under test. For example, sampling of a sine wave of amplitude "A" results in an amplitude distribution illustrated in Figure 16. Pulse histograms are particularly useful in the analysis of radar scan characteristics and are naturally suited to digital processing. An advantage is that several pulses in a radar scan may be missed with little degradation in the histogram. The result is similar to integration in typical radar receivers where several pulses are integrated over the radars observation time. It is possible with a histogram generating system to miss pulses and still complete the signal identification even though the

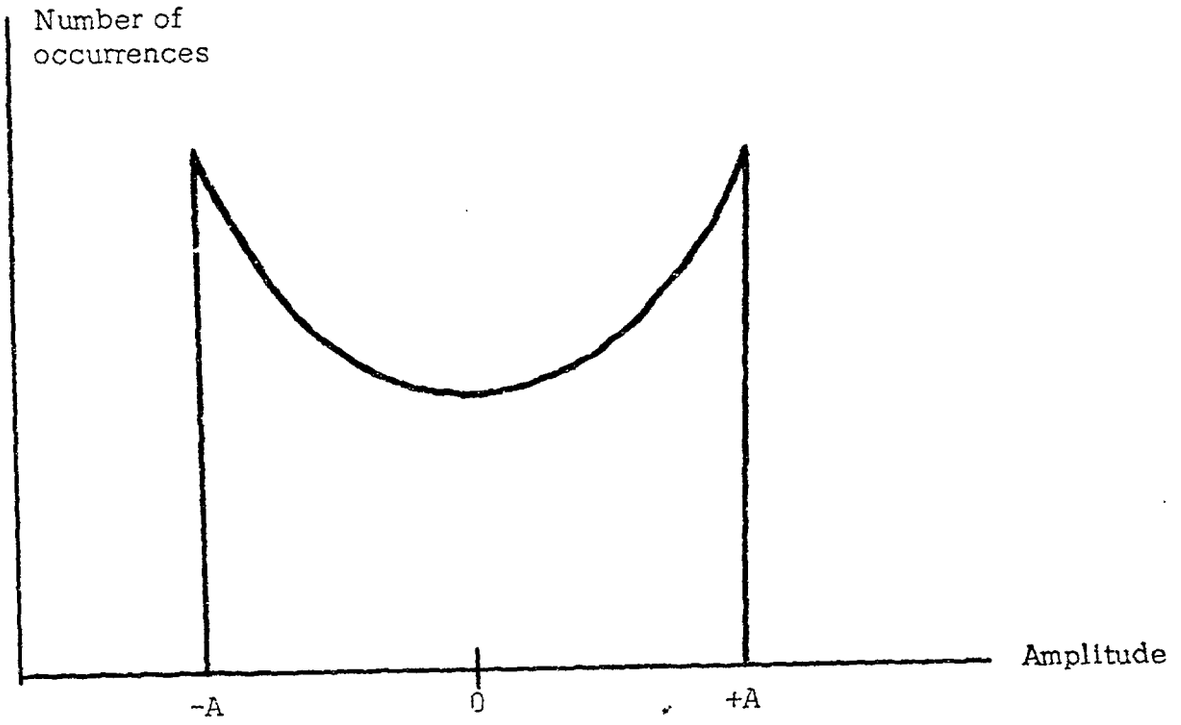

Figure 16. Histogram of Sine Wave

averaging process on other parameters such as PW and PRF many create significant errors. Techniques such as histogram analysis may serve to overcome some of the difficulties of computer threat signal sorting and analysis.

F. THE EFFECT OF DISPLAYS ON PROBABILITY OF INTERCEPT

A frequently overlooked problem area in ECM intercept systems is the display of data once properly collected. Without proper display it is impossible for the operator to make critical decisions important to the successful completion of the mission. For every signal missed or action delayed because of inadequate display one may as well have not intercepted the signal. It is obvious, therefore, that if the system intercept probability is to approach unity, the operator, as part of the system, must be provided with information in an orderly, efficient, timely, and easily recognizable form. In dense ECM environments the input data rate generates an equally dense output data rate. Output equipment in the form of frequency spectrum displays, pulse analyzers, direction finding equipment, signal spectrum analyzers and other special purpose analysis equipment are utilized by operators. With a trend toward wide-band systems utilizing IFM's there is a need to consolidate display instruments so that ideally a single display may handle all analysis functions. Currently, IFM's use Polar frequency displays.

IV. ADDITIONAL METHODS USED TO IMPROVE PROBABILITY OF INTERCEPT

In addition to the methods discussed in the previous section there are several methods one may use to increase the system POI. To counter the extreme time to search the entire rf band when using intermediate scan rate superheterodyne receivers, signals may be grouped into priority blocks of frequency based on intelligence reports. The receiver can then be programmed to search only priority blocks, maximizing POI for the priority signals. One must realize, however, that the POI for signals outside the priority blocks are severely degraded. However, based on the definition of POI earlier in this report, POI is unity so long as the system accomplishes the mission. If the mission is to intercept certain priority signals at the expense of others then the mission is accomplished and POI is unity by definition.

Where the direction to threat is known, one may establish an azimuth zone commonly called the "threat axis". Using directional antennas one can then fix the antenna azimuth along the threat axis eliminating the need for angle scan thus increasing POI. This method was easily adapted to the Vietnam situation where naval aircraft approached the coast from the South China Sea. ECM and attack aircraft then had well defined directions to threats which allowed one to establish a threat axis.

Against scanning type radars, ECM system POI is degraded because of the large percentage of time that the transmitting antenna is not directed

toward the ECM intercept platform. One need only intercept side and back lobes of the transmitted beam to significantly increase POI. The most obvious solution is to decrease transmitter to interceptor range to the point where 100% intercept is achieved. Unfortunately, most ferret receivers are directed against targets hostile to over flight or border violations leading one to establish intercept ranges typically greater than 20 miles. Alternatively, one must increase system sensitivity to allow interception at normal range. Postulating a parabolic transmitting antenna, one finds that side lobes are typically 20-30 dB below peak. [9] Rf pre-amplification, parabolic or horn high gain antenna may be used to provide the increased gain required.

Where many frequency bands must be covered by a single scanning receiver, "folded rf" may be used to decrease scan time. "Folded rf" is a method used to fold many rf bands into a single rf band allowing a shorter scan time per band. Figure 17 illustrates the scheme in block diagram form for a three octave rf bandwidth system. One will note that the single tuner now tunes the 500-1500 MH_z range three times, effectively covering 8 GH_z of rf bandwidth in the scan time for 3 GH_z, or a 2.6 reduction in scan time.

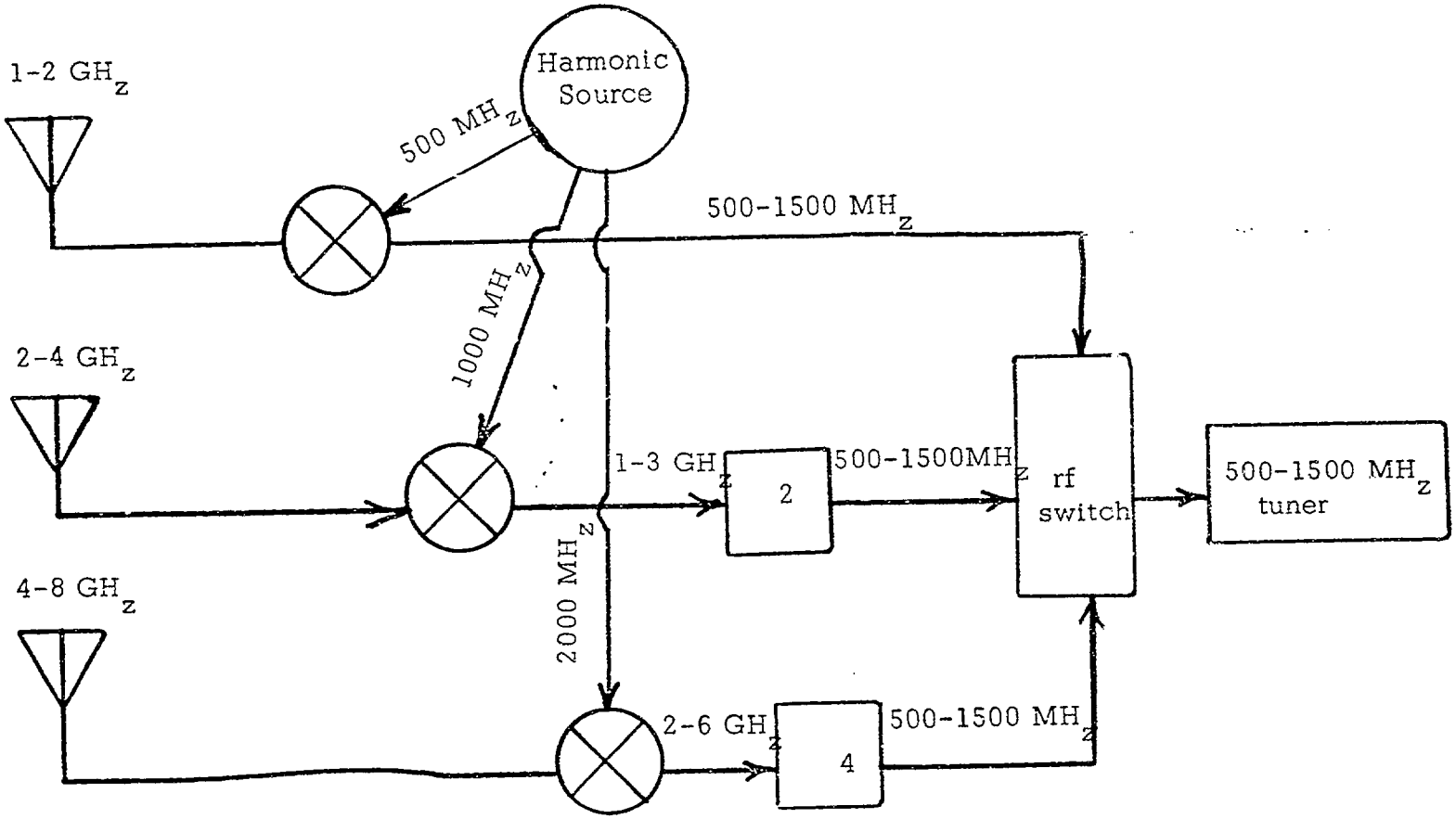

Figure 17. Sample Folded rf Intercept System

V. SYSTEMS THAT ATTAIN UNITY PROBABILITY OF INTERCEPT

A. GENERAL

The rapidscan and microscan receivers covered in previous sections provide unity probability of intercept against signals that the systems were designed to intercept. It was demonstrated that both the rapidscan and microscan receivers are not capable of unity POI against all signals in band, especially for systems that require highly directional antennas for sensitivity or direction finding. The wide-open rf crystal video type receiver is capable of unity POI provided signal strength is sufficient. It was noted, that the sensitivity of wide-open receivers is low compared to superheterodyne receivers in the absence of high gain antennas or rf preamplification. In addition, wide-band receivers do not provide a frequency resolution capability which limits their application to systems where unity POI is necessary and frequency information expendable. The design criteria for the receivers above was covered in previous sections and will not be repeated here.

This section will cover the two-tuple, IFM, and acoustooptic type receiving systems. Emphasis will be on the acoustooptic device.

B. TWO-TUPLE RECEIVER

A unique channelized receiver using significantly reduced numbers of filters compared to a typical channelized receiver is the two-tuple receiver. The two-tuple provides the advantage of instantaneous frequency

measurement with a compartmented type frequency resolution, eliminating the polar type frequency display associated with other IFM systems. The main features of the two-tuple receiver are outlined in block diagram by Figure 18. Phase modulating signals A and B are input to the TWT helix causing a single frequency on the helix of TWT #1 to produce phase modulation of frequency A and harmonics of A in TWT #1. A single frequency on the helix of TWT #2 produces phase modulation of frequency B and harmonics of B in TWT #2. The high pass filters reject low frequency mixing products that fall out of band (rf) between input signals and the phase modulation frequencies and their harmonics. Filter bank A has a total width equal to the phase modulating signal A while filter bank B has a total width equal to the phase modulating signal B where B is A plus 4 times the frequency resolution desired by the system. The number of filters in each bank depends upon the frequency resolution desired by the system. If one desires a resolution of $\pm$ R MH_z, the number of filters is equal to

$$\#\text{FILTERS} = \frac{\text{PHASE MODULATION FREQUENCY}}{2R} \tag{34}$$

where the numbers are chosen to avoid fractions and each filter band is overlapped in frequency by R MH_z. To provide the required overlap, it is required that the second filter bank be 4R MH_z plus the width of the first filter bank due to the difference in frequency of A and B. Filter arrangements are depicted in Figure 19. Filter bank B will require two additional filters to provide a total width equal to the B phase modulating

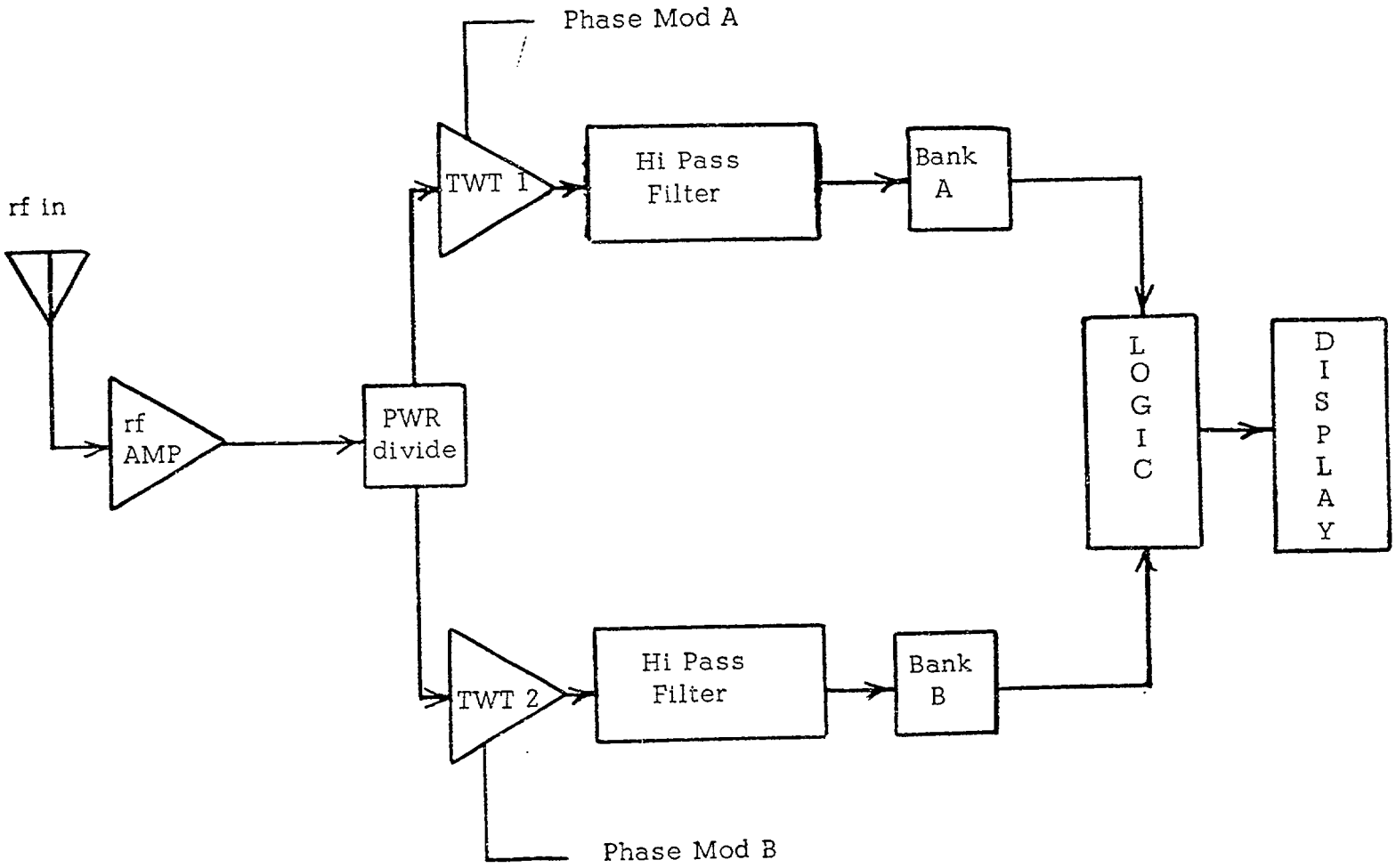

Figure 18. Two-Tuple Receiver

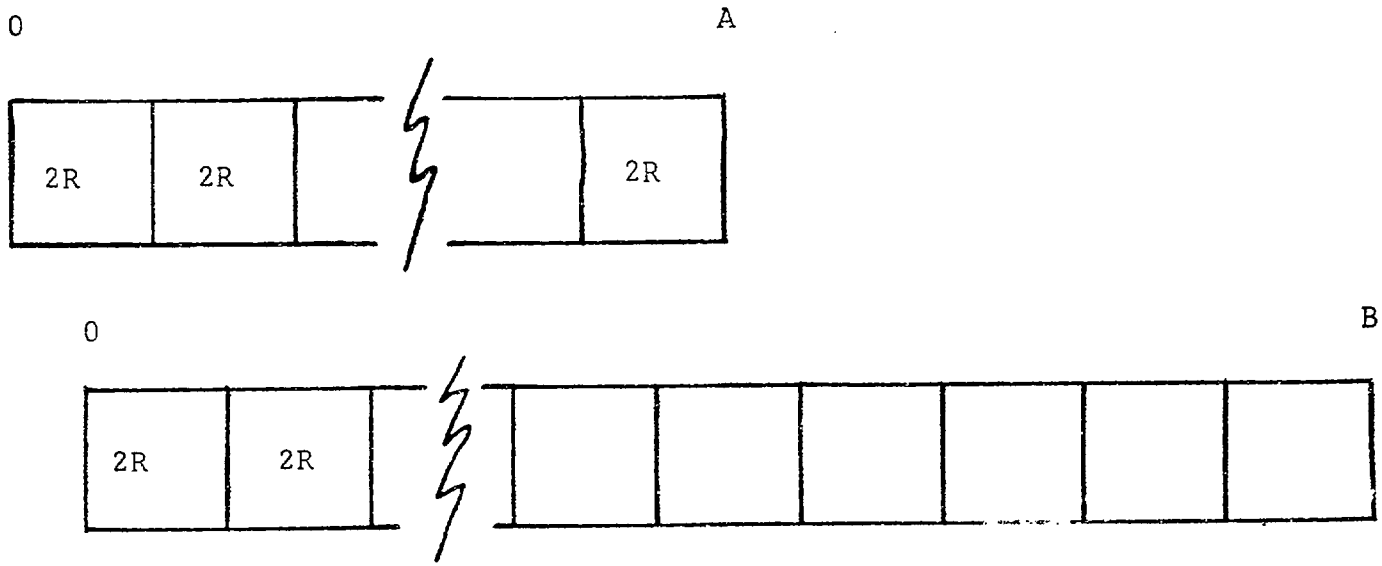

Figure 19. Two-Tuple Receiver Filter Banks

frequency. From the input frequency range one can select values of A and B, then calculate mixing sum and difference products, including harmonics, for representative frequencies across the band. By properly selecting the low end frequency of the first filter one will find that only one filter in the bank will respond to an input signal. The response will be due to either signal $\pm$ fundamental or signal $\pm$ one of the harmonics. Once one establishes one filter bank frequency beginning point the other is given by simply adding R to the frequency starting point of the first filter. In the second filter bank one will find that a single filter responds but at a different position than the first bank because of the frequency separation between A and B and the R MH_z offset between filter banks. Since only one filter in each bank responds to an input signal it is rather straightforward to construct a logic network that will provide an output unique to a signal falling in a $\pm$ R MH_z range. One will note that a normal channelized receiver would require

$$\#\text{FILTERS (NORMAL)} = \frac{\text{rf BANDWIDTH}}{\text{FREQ. RESOLUTION}} \tag{35}$$

to provide the desired resolution. The two-tuple receiver on the other hand requires

$$\#\text{FILTERS (TWO-TUPLE)} = \text{'A' BANK} + \text{'B' BANK}$$

to meet the required resolution. For example assuming a 4,000 MH_z rf bandwidth with 15 MH_z resolution, the normal channelized receiver would require 267 filters while the two-tuple with frequency A equal to 420 MH_z and B equal to 480 MH_z (typical) one would require 14 + 16 = 30 filters, a reduction of over eight times. [36]

The AN/SLQ-12 ECM system utilizes the two-tuple concept. Display is through an array of indicators, illuminating whenever a signal in a particular 15 MH_z portion of the rf spectrum is detected.

By providing rf switching at each filter, one could obtain rapid individual signal analysis by switching the filter output to a detector followed by a pulse analysis system. A channelized output like the two-tuple receiver presents a problem to the operator in that he must scan a relatively large area for illumination of the signal indicators. By providing a holding circuit for the illuminators, narrow pulsewidth signals could be detected but an analysis could not be made unless constant monitoring and detection of each channel was accomplished. By providing detectors at each 15 MH_z filter, one could drive a multiple channel strip chart recorder to provide real-time analysis and detection. The operator could watch the much smaller strip chart for signal arrival and be provided with a rough pulse width, pulse repetition interval, scan characteristics, and an indication of frequency hopping or frequency agile radars. Where precise emitter characteristics were desired, the operator could switch any output to a high quality pulse analysis and recording system.

The two-tuple responds favorably to all modulation types. Pulsed FM or chirp signals are detected by observing the illumination of adjacent frequency indicators provided the frequency deviation is greater than R MH_z. CW signals and normal pulsed signals will illuminate a single frequency indicator. Frequency agile radars will be displayed as alternating indicator illumination and a distinct hopping or sweeping through

the display. Simultaneous signals in a particular 2R MH_z filter simply generate mixing products within that filter so that interfering and ambiguous signals do not appear in other filters. If the frequency deviation of a chirp signal is not greater than 2R MH_z the signal will appear as a normal pulsed signal unless FM demodulators are provided at each filter output.

Similar to other wide-band systems, the two-tuple receiver has low sensitivity unless one adds rf preamplification or high gain antenna systems. This low sensitivity combined with expensive filters serves to reduce the attractiveness of the two-tuple receiver. It was noted earlier in this report that the cost of rf components is undergoing a continual reduction due to miniaturization and integration. Provided the cost for high quality filters is decreased to a point where they become attractive for production ECM systems, the two-tuple will remain cost ineffective compared to other systems that attain a similar end product, that of instantaneous frequency monitoring with unity POI.

C. INSTANTANEOUS FREQUENCY MEASURING RECEIVERS

1. General

Instantaneous frequency measuring receivers classically known as the microwave rat race receiver provide unity single pulse POI while instantaneously giving the frequency of the received signal. The heart of an IFM is an element that is in some way frequency sensitive. Most common is a receiver using quadrature hybrid junctions.

A phase separation between two signals of equal amplitude can be detected with a summing or differencing circuit. Let the two signals be represented by $A\cos(\omega t)$ and $A\cos(\omega t + \alpha)$.

Define

$$V_y = A\left[\sin(\omega t + \alpha) - \sin \omega t\right] = 2A \sin \frac{\alpha}{2} \cos\left(\omega t + \frac{\alpha}{2}\right) \tag{36}$$

$$V_x = A\left[\cos(\omega t + \alpha) + \cos \omega t\right] = 2A \cos \frac{\alpha}{2} \cos\left(\omega t + \frac{\alpha}{2}\right) \tag{37}$$

where V_y and V_x are the x and y voltage components respectively. In block diagram form, Figure 20 illustrates a basic IFM receiver that will produce the desired mathematical relationships, V_x and V_y. If one forms the ratio V_{y/V_x} the result is the tangent of 1/2 the phase difference between the two signals. By applying the two voltages directly to the vertical and horizontal plates of a CRT one obtains a straight line inclined at a slope $\alpha/2$ and of length proportional to amplitude A. To construct an IFM one must convert frequency differences ω into phase differences . By delaying the signal in one channel by an amount τ seconds, the delayed portion lags the other channel by a phase difference of $\alpha = \omega\tau$. The CRT then displays a straight line where slope is directly proportional to input instantaneous frequency. [34] The implementation of an IFM receiver makes use of quadrature hybrid junctions (QHJ) for the difference and summing functions required. Using power splitters, a microwave delay line, quadrature hybrid and a CRT a basic system appears in Figure 21. The system illustrated in Figure 21 is commonly known as the linear polar display IFM. Using only linear components permits the

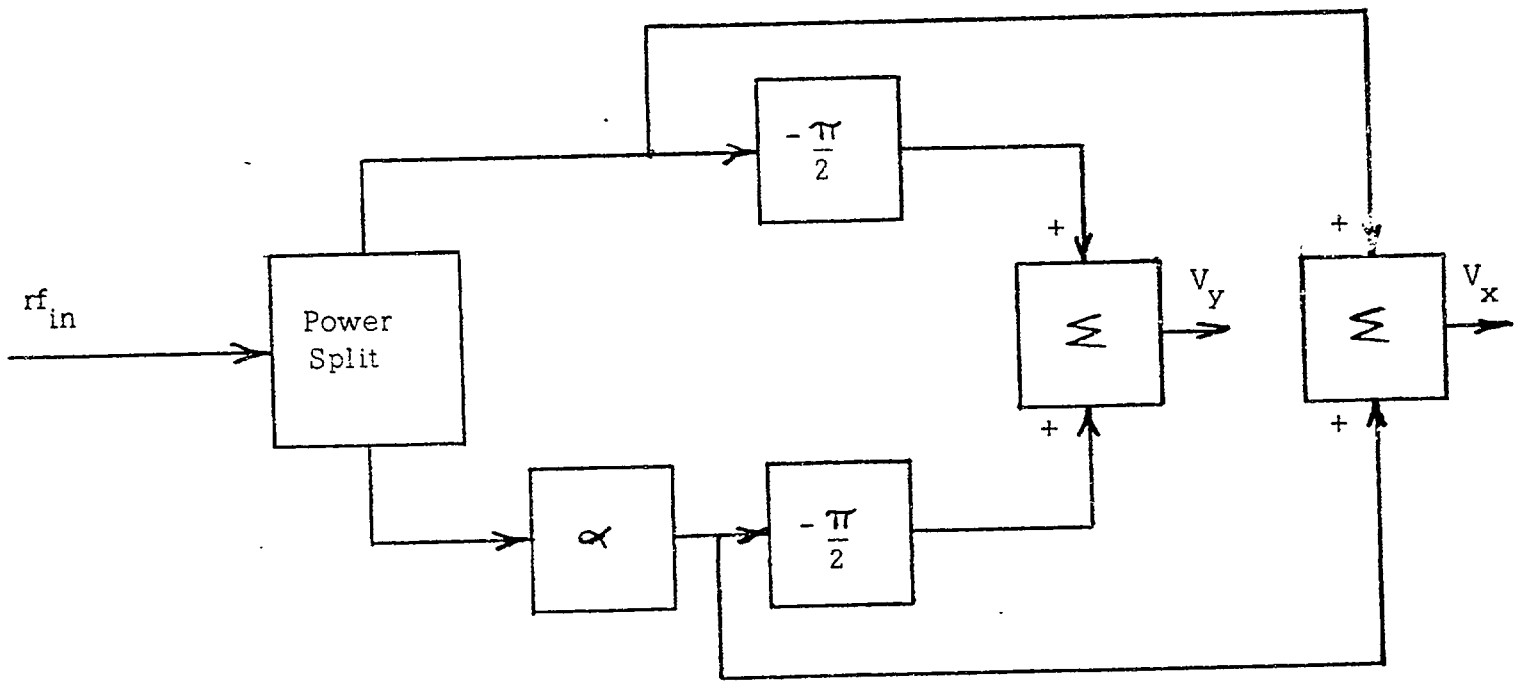

Figure 20. Basic IFM Receiver

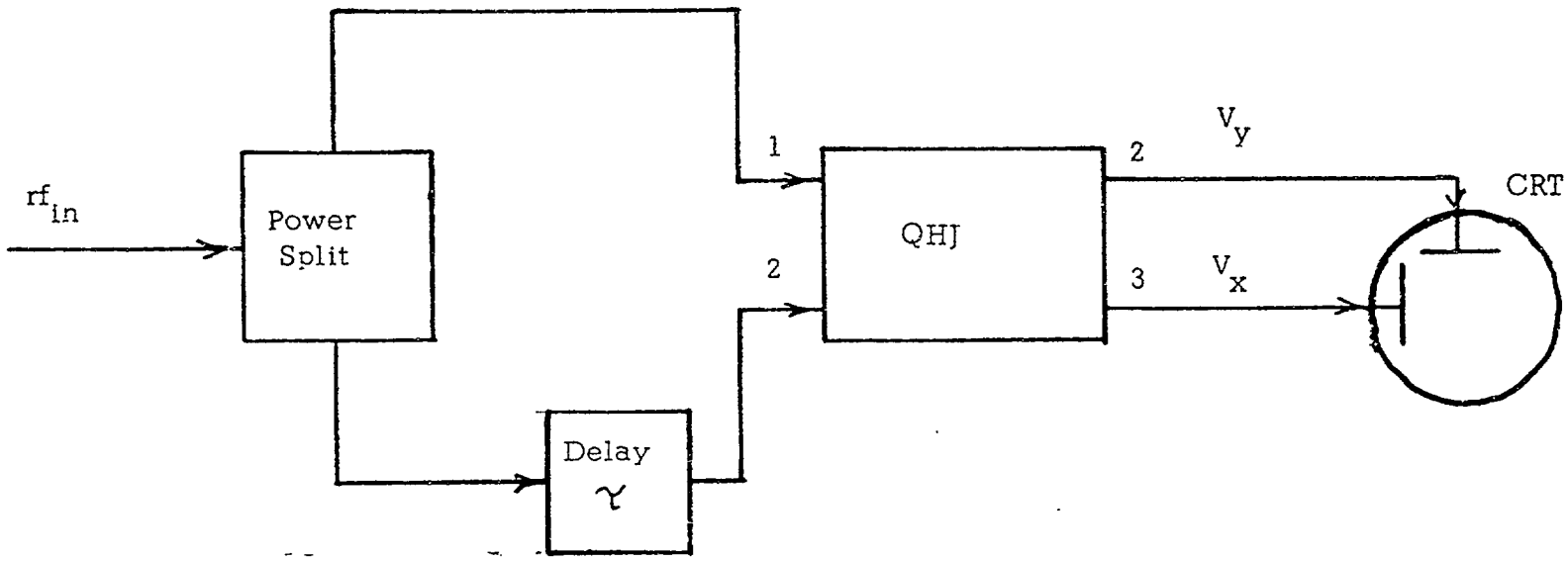

Figure 21. Simple Linear Polar Display IFM

IFM illustrated to obtain bandwidths of an octave or better. An advantage of a system of this type is that one obtains a frequency display without the need for detectors. At GH_z frequency ranges down conversion is generally required to permit display on the CRT with mixing taking place prior to the QHJ.

The linear polar display (LPD) IFM is susceptible to display ambiguity when two or more signals arrive simultaneously. Two sinusoidal (CW) signals produce a parallelogram type display where the sides of the parallelogram are inclined at slopes indicative of the instantaneous frequency of each signal, and length indicative of the amplitude of each signal. In general, 'N' CW signals would produce a polygon of N pairs of parallel sides with each pair indicating instantaneous frequency and amplitude. So long as the CW signals coexist a large part of the display is degraded for non-CW signals at other frequencies. The effect of the parallelogram display is similar to noise jamming in a radar display.

Frequency modulated signals are displayed as a bow-tie where the total arc swept by the display is an indication of frequency deviation and the length of the display an indication of amplitude. If a signal is of sufficient strength to be received continuously, the FM signal display effectively jams a sector of the display reducing the probability of detecting other signals in the same sector. One must note that this limitation is a function of the display not of the receiver.

The display limitations noted above reduce the application of the LPD IFM to uses other than ECM receivers. An improvement will be presented in the following section.

An improved IFM usable for ECM receiver applications is the postdetection polar display (DPD) IFM. Improved electrical symmetry throughout the circuit allows a considerable improvement in bandwidth to beyond an octave. Significant in the DPD IFM is that signals are displayed as dots displaced from the center of a CRT. Signal amplitude is indicated by distance from center and frequency by angle measured from horizontal. The advantage of the dot display is that the bow tie type display that reduced display capability in the linear display IFM is eliminated. A basic version of the DPD IFM is illustrated in Figure 22. Frequency determination is made by using logarithmic amplifiers and summing circuits to form the ratio of signals from the two channels. Alternatively, a CRT could be used to form the summing and ratioing functions by taking outputs prior to the log video amplifiers. Single unit systems obtain frequency measurement accuracies of 1% under laboratory conditions and 3-4% in field tests. Using two systems in quadrature allows one to obtain better than 1% accuracy provided signal-to-noise ratio exceeds approximately 15 dB.[37] Improvement in frequency measurement accuracy is provided by the additional balancing of the circuit when additional quadrature hybrids are used. A complete system is illustrated in Figure 23. The output of the DPD IFM is a constant voltage independent of amplitude and proportional to the frequency of the input signal. Amplitude information can be provided by adding a detector and log video amplifier in parallel with the frequency sensing system. The two outputs may be combined to drive a display or

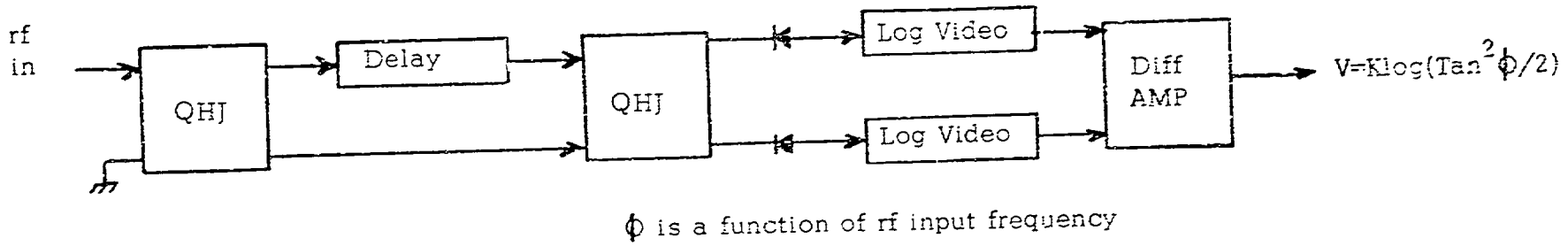

Figure 22. Basic DPD IFM System

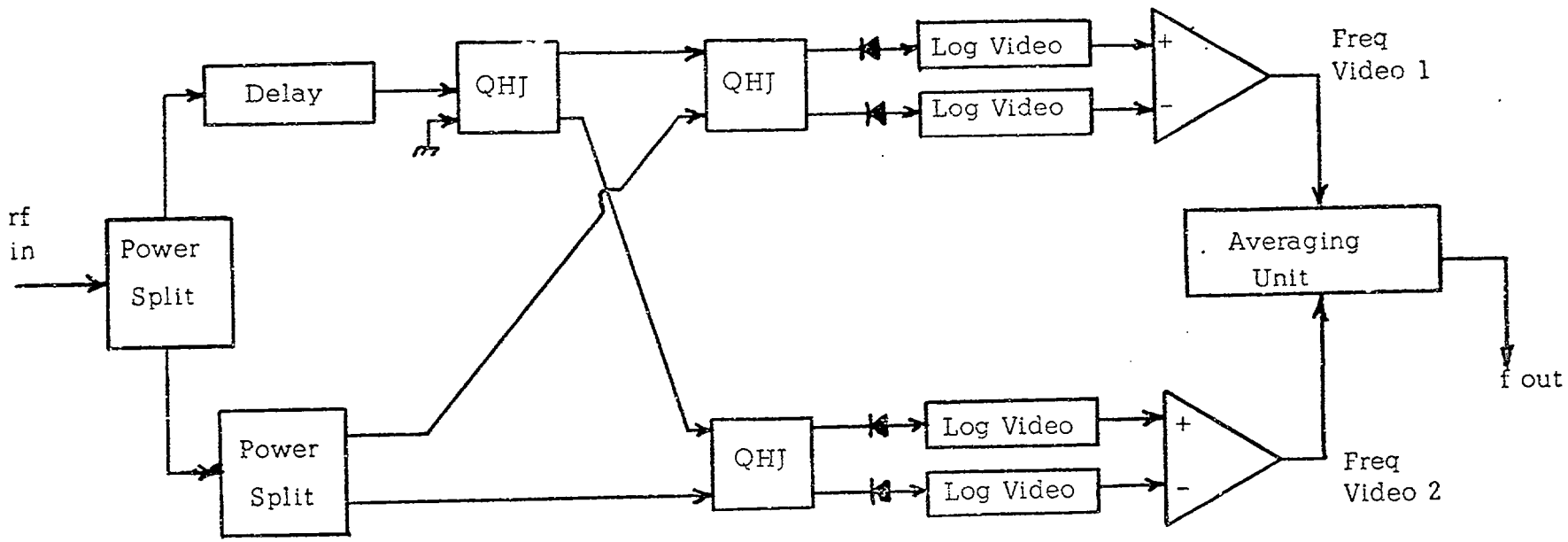

Figure 23. DPD IFM System

the frequency outputs may be averaged to provide a digitized representation of frequency for input to a digitized signal processor.

Systems of the type shown in Figure 23 are susceptible to interference generated in the QHJ when two signals arrive simultaneously. Simultaneous signals cause an averaging to take place in the microwave discrimination section of the IFM (QHJ) and results in the display of spurious signals. The spurious signal problem is especially severe when both signals are CW types. Two CW signals operating simultaneously generate a display that is the average of the two individual signals. Standing alone, the spurious signal response is the single most distracting feature of the IFM. One method that can be utilized to avoid display of spurious signals is to provide a means of detecting simultaneous signals and inhibiting the display during the period the signals are coincident. If the signals are CW type and of long duration the system may inhibit the display for an exceptionally long time period. Such a situation could occur when attacking aircraft are illuminated by a multi-frequency CW radar operating in a defensive system. Probe Systems PRS-3100 IFM receiver and display system combines an IFM receiver with a TRF receiver. Automatic detection of simultaneous signals is provided eliminating this source of measurement error. It must be noted that by inhibiting the display during simultaneous emitters, one is actually reducing POI for the interfering signals. The combination of an IFM and TRF in a single unit provide single pulse POI of unity and an analytical capability from the TRF through queing from the IFM. [37]

Similar to most wideband systems the sensitivity of the IFM is no better than a crystal video receiver with the added degradation of 3 dB due to the use of power splitters and hybrids. Using the TRF with the inherent added sensitivity does not actually help POI since the IFM ques the TRF for analysis purposes. If one relied on the TRF to intercept signals of interest the POI for the system would be no better than that attainable by the TRF.

By combining the IFM receiver with various combinations of antenna systems and superheterodyne scanning or manually tuned receivers, a system with near ideal intercept parameters can be obtained. Through various combinations, the system can direction find, perform pulse train analysis, and remain open in frequency to immediately detect short-duration signals or detect any changes in emitter operations such as starting, stopping or changing frequency. An automatic computer-based system or manual operator maintains a continuous picture of the ECM environment from which to select countermeasures or signals for processing.

2. Omni IFM, Omni Superheterodyne

IFM receivers using omni antennas are able to intercept the main lobes of target radars and the side lobes of nearby radars. A superheterodyne with omni antenna can be qued by the IFM to analyze selected signals in detail. The overall sensitivity of such a system is low and typically will not allow reliable intercept against radars in excess of 30 miles. The low sensitivity results in a decreased input data rate allowing one to use processors with less storage capacity or slower speed. Scan

analysis on selected radars can be obtained from the IFM since only main lobes will generally be received. A system such as the one above is basic and may be useful in platforms with a limited radar horizon, i.e., ships.

3. Omni IFM, Direction Finding Superheterodyne

By adding a DF antenna system to the superheterodyne, the system is able to DF in addition to providing the services outlined above. The superheterodyne receiver in this application has an increased POI over similar systems in the absence of the IFM because of the queing provided by the IFM. If one provided an omnidirectional back-up antenna for the superheterodyne, a reasonable high POI would still be provided by the system provided the superhet scan rate met the criteria established in preceding sections of this report. A capacity for back-up in the event of a partial system failure is a desirable feature. Considering that the omni antenna for the IFM would be available in the event of an IFM failure, one need only provide rf patching to accomplish the capability.

4. DF Acquisition, Omni Analysis

With the high gain DF antenna used with the IFM, radar side and back lobes at long range may be intercepted. This technique facilitates the detection and correlation of emitters in a multi-emitter site and can assist in platform identification when the platform has multiple emitters. All radars in a particular azimuth cell will be intercepted by the IFM. Data rates will be reduced by the factor that only radars in the DF beamwidth are intercepted. The superheterodyne receiver will have

a sensitivity only slightly less than the IFM plus DF antenna because of its inherently higher basic sensitivity due to its narrow bandwidth. This enables the superhet to analyze all signals qued by the IFM without significant sensitivity loss on the part of the omni equipped analysis receiver. One must note that strictly defined, system POI is no longer unity but is degraded by the DF antenna search rate. The time to intercept, therefore, is the scan time for the DF antenna. A system of this configuration is particularly able to keep track of a wide area. Even if target radars do not scan, the increased sensitivity of the IFM allows intercept on back or side lobes. During the period the DF antenna is scanning for new signals, the superhet is able to detect signals over a wide band. By properly selecting the DF antenna scan rate and superhet RF scan rate, one can achieve near unity POI. One should compare this result with the near zero POI obtained with systems that rely on a scanning superhet and scanning DF antennas for signal acquisition. When scanning in frequency, frequency agile radars appear as multiple signals. An IFM on the other hand is able to track the jumps in frequency and immediately determine frequency hop characteristics. [30]

5. IFM's Versus Wide Band Receivers

It has been pointed out that one of the main reasons for selecting IFM's over the wide band system is the frequency resolution provided by the IFM. Studies of the electronic Order of Battle indicate that very few signals cannot be identified through parameters other than frequency. Failure to identify the few signals remaining is due to an

unresolvable ambiguity between signals of identical parameters except for frequency. It has been suggested that a wideband IFM type frequency resolving capability is not necessary and rather, results in an unnecessarily high output data rate. An alternate method is to utilize a dedicated processor or computer similar to ATAC-8 or Pointer to de-interleave and analyze pulse trains using the output of a wideband crystal video receiver with RF preamplification. One would provide the processor with a sufficiently large reference file so that it could identify emitters and be aware of emitters where an ambiguity may exist. By providing a simple digitally tuned superheterodyne receiver controlled by the computer, the computer can flag the superhet to check one or more frequencies to resolve ambiguity. Since the number of ambiguities are small, the look up time in the computer files will be small and the process of frequency ambiguity resolution rapid. Significant in the system is an avoidance of the frequency ambiguity situation in the IFM when simultaneous signals arrive.

D. ACOUSTOOPTIC RECEIVERS

1. Background

Acoustic energy launched into a medium causes a refractive-index change via the photo elastic effect. The refractive-index change results in a periodic variation in refractive-index across the device with period equal to the period of the acoustic wave and amplitude proportional to the sound amplitude and the magnitude of the photoelastic effect in the medium. [38] To light energy, the periodic variation in refractive-index

appears as a phase grating that is capable of diffracting the light in one or more directions. Devices utilizing this phenomena of interest in this study are acoustooptic light deflectors or Bragg cells.

Until the advent of lasers with their monochromatic output, precision acoustooptic deflectors were unavailabie. Laser sources allow one to establish exact reference points in the deflected output so that only acoustic disturbances result in a beam deflection. Prior to lasers, the best sources contained enough incidental FM to cause the deflection angle to be a function of FM plus acoustic signal where the FM was not precisely trackable.

The basic geometry of the interaction between the light and acoustic waves is given in Figure 24 where K and Ω are the wave number and angular frequency of the acoustic wave and k and ω are the wave number and angular frequency of the light wave. Uchida, et. al. [38] and Chang [39] demonstrate that first order diffraction is dominant when the incident angle θ is equal to the Bragg angle θ_B, given by

$$\sin \theta_B = \frac{\lambda_o}{2n\Lambda} \tag{38}$$

where

Λ = acoustic wavelength in the medium

n = refractive-index of the medium

λ_o = free space wavelength of the optical wave

In general multiple orders of diffraction may occur. If the width of the acoustic device (L) is large compared to the ratio Λ^2/λ ,

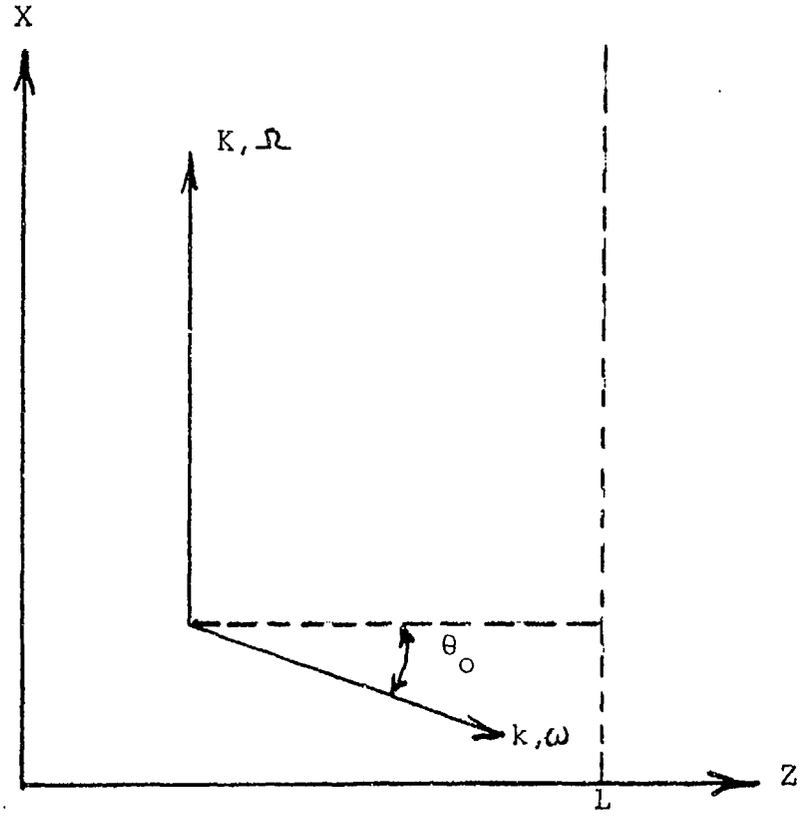

Figure 24. Basic Acoustooptic Interaction

where λ is the wavelength of the light wave, the amount of energy coupled to higher diffraction order will be reduced and added to the zero and first order modes. [40] This region appropriately is known as the Bragg region. Equation (38) demonstrates that the deflection is dependent upon the acoustic frequency provided the light frequency is fixed. By injecting acoustic signals of varying frequency one obtains an output at various angles depending on frequency. In this manner the acoustooptic device acts as a frequency meter provided the deflected light beam is detected at each angle of deflection. Figure 25 illustrates a typical acoustooptic deflector.

In the design of acoustooptic deflectors, there are three main parameters: (1) deflection efficiency, η , (2) random access time, τ , and (3) number of resolvable spots (N). The number of resolvable spots is specified in terms of the Rayleigh criteria, familiar to radar engineers as the separation required in azimuth for two targets to be detected. The analog to the acoustooptic device is valid in that the diffracted energy distribution follows a $SINC^2X$ energy distribution similar to a parabolic antenna pattern. The $SINC^2X$ distribution can be utilized to select the number of Rayleigh criterion resolvable spots based on signal level differences required by adjacent detectors or cross talk considerations.

In the deflector, the concern is with the ratio of the angular scan capability of the deflector to the minimum resolvable angle. From Figure 25 one notes that the angle between the undeflected and diffracted beam is $2\theta_B$. For normal deflector operation, small angles are involved

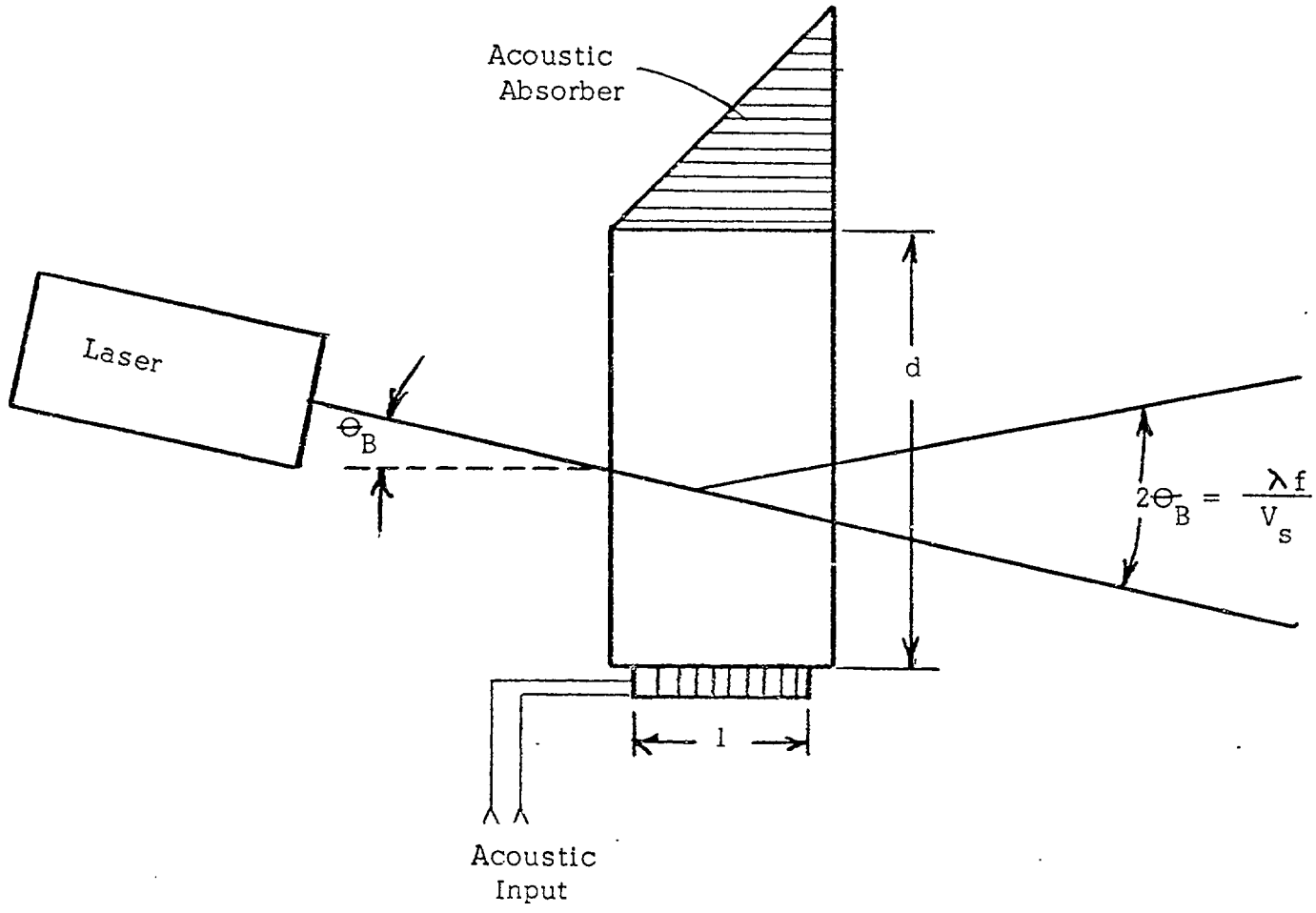

Figure 25. Acoustooptic Deflector

and the angle can be approximated by

$$2\theta_B = \frac{\lambda f}{V_S} \tag{39}$$

where V_s is the acoustic velocity in the medium. The ratio is limited by the deflectors limited acoustic aperature. One finds that the acoustic aperature must be large to establish validity of operation in the Bragg region, but must be reduced to increase bandwidth. [39] It can be shown that the total angular scan capability of the deflector is given by

$$\Delta(2\theta_B) = \Delta\left(\frac{\lambda f}{V_S}\right) = \frac{\lambda}{V_s}\Delta f \tag{40}$$

where Δf is the optical bandwidth of the deflector. The optical bandwidth is found to be dependent upon the optical transducer, and the Bragg angle bandwidth. Chang [39] demonstrated that an approximate 3 dB bandwidth is given by

$$\Delta f = \frac{1.8\, n\, V_S^2 \cos\theta_B}{\lambda_o f_o L} \tag{41}$$

where f_o is the free space optical frequency. When light of uniform intensity and coherence is applied across the aperature d, the smallest resolvable angle given by the Rayleigh criterion is

$$\theta_{min} = \frac{\lambda}{d} \tag{42}$$

The number of resolvable spots is then given by the ratio of equation (40) and equation (42)

$$N = \frac{\Delta(2\theta_B)}{\theta_{min}} = \frac{\Delta f\ d}{V_S} \tag{43}$$

If one defines the random access time of the device as $\tau = \frac{\Delta f}{V_s}$, equation (43) reduces to $N = d\tau$. Acoustooptic deflectors are compared by the time bandwidth product $d\tau$ similar to the time bandwidth product of i-f amplifiers in radar receivers.

Δf is a result of both the electrical and mechanical quality factors (Q). The mechanical Q is a function of bonding of transducers to the Bragg cell where differences in mechanical, hence acoustic impedenc s exist. The electrical Q is a function of transducer capacitance-radiation resistance and the electrical parameters of the material.

The bandwidth of a deflector depends upon the bandwidth of the Bragg angle. This bandwidth is established to give a measure of the range over which Bragg diffraction occurs. Operation outside of this range results in diffraction orders other than Bragg. Heynan [40] defines Bragg bandwidth as $\pm(1/2)\ \Lambda/L$. For a given acoustic center frequency, this limits the acoustic transducer length.

Random access time is a measure of how rapidly the device can respond to a frequency different from a frequency already present. The time for the response is simply the time required for the new frequency information to propagate across the cell aperature.

The deflection efficiency is defined as the fraction of incident laser beam that is deflected using one watt of electrical drive input power. Transducer piezoelectric coupling efficiency, bandwidth broadening or acoustic impedence matching film layer insertion losses, and the acousto-optic scattering efficiency of the medium, all affect overall deflection

efficiency. The acoustooptic scattering efficiency of the medium can be shown to be related to basic material properties, the frequency of incident laser light, cell dimensions and acoustic power.

2. Acoustooptic Material Figures of Merit

It is convenient to compare acoustooptic materials on the basis of their ability to efficiently deflect light beams. Define the acoustooptic figure of merit, M_2, as

$$M_2 = \frac{n^6 \rho^2}{\rho V_s^3} \tag{44}$$

where n is the refractive index, P, the photoelastic constant, ρ, the density and V_s the acoustic velocity in the medium. [38,39,40] The fraction of light scattered can be shown to be

$$\% \text{ scattered} = \sin^2 (\eta)^{1/2} \tag{45}$$

where η is directly proportional to M_2. From equation (41) one observes that Δf is proportional to nv^2. If one defines a figure of merit, M_1, as

$$M_1 = \frac{n^7 \rho^2}{\rho V_s} = M_2 \eta V_s^2 \tag{46}$$

then optimization of M_1 will yield an optimum efficiency-bandwidth product for the device. M_1 is used when the minimum height of the transducer is constrained because of construction or impedence limits. A factor M_3 is used when the transducer size is not limited. In the design of wideband systems power density may be the limiting factor. In this case it is found that a figure of merit M_4, given by

$$M_4 = M_2 (n v^2)^2 \tag{47}$$

is useful. The reader will note that the figures of merit may all be derived from M_2 and basic material properties. Throughout the literature it is common for the figures of merit to be referred to the values obtained for fused silica where M_{2R} is defined as unity. Fused silica is the "benchmark" material by which all other materials are judged. [40]

Acoustic attenuation is the next important property to consider in the selection of acoustooptic materials. The acoustic absorption coefficient α is given by

$$\alpha = \frac{\gamma^2 \Omega^2 K T}{\rho V_s^5} \tag{48}$$

where

γ = Grüneisen's constant

K = thermal conductivity

T = temperature

Using equation (44), one can demonstrate that

$$\alpha = \left(\frac{\gamma^2 \Omega^2 K T}{V_s^2 n^6 p^2} \right) M_2 \tag{49}$$

One observes that materials with high refractive figure of merit will have the greatest acoustic attenuation factors.

The choice of materials becomes a trade-off in the optimization of deflection efficiency and attenuation. An important factor to consider, therefore, is the availability of high optical quality materials in quantities large enough to allow device fabrication. Fused quartz is a popular

material because of its high optical quality, low acoustic attenuation and availability of large-size elements. Fused quartz is capable of large numbers of resolvable spots and can be used with carrier frequencies up to 350 MH_z before acoustic attenuation becomes a factor in most devices. Reference 38 provides an excellent presentation of the properties of selected acoustooptic materials and the chemistry involved in predicting selected material properties. Reference 40 provides a simplified discussion of selected materials from an applications point of view.

The search for an ideal material is continually underway. Materials Processing Developments onboard Skylab indicate the possibility of a new generation of materials when the first full-time space stations are orbited. Of particular significance in space processing is the absence of gravity caused convection currents in molten materials. The absence of convection currents results in a greatly improved crystallization process where materials crystallize in shapes and orientations dependent upon internal atomic or molecular forces only. A much more uniform crystal is formed in space than can be achieved on earth with electrical and optical qualities never before achieved. Experiments using Gallium Arsenide, an important acoustooptic material, demonstrated that superior quality crystals can be obtained in space. It is important to note that materials immiscible on earth because of gravitational separation, undergo no separation in space but remain mixed during solidification. This presents an entirely new picture to the materials scientist in that materials never before considered may now be processed.

One of the most severe restrictions to the operation of the Bragg cell microwave receivers is the narrow bandwidth achievable. Approximately octave bandwidth is attainable in current devices at an acoustic frequency of approximately 250 MH_z. At higher frequency ranges input rf bandwidths of 4 GH_z or better are typical. Methods must be provided to restrict rf bandwidth or alternatively provide multiple cells to cover the spectrum under surveillance. Acoustic bandwidths up to 700 MH_z have been achieved using $LiNbO_3$ for the Bragg cell. Advances in cell technology and recent developments in transducer technology indicate that GH_z bandwidths are achievable. [39]

Once the basic Bragg cell is selected, one is faced with having to launch an acoustic wave into the cell. Acoustic transducers provide the interface between the electrical driving signal and the mechanical generation of the acoustic wave. The transducer must be designed with a high coupling efficiency to limit heat generation within the device and with a bandwidth sufficient to provide full cell bandwidth utilization. Both factors are affected by the methods used to bond the transducer to the cell. Both acoustical and electrical impedance matching is generally required. Matching is accomplished through various techniques including the use of thin films. [38] Thin-plate piezoelectric transducers bonded with epoxy resin are found to be the best approach currently available. Due to the low mechanical impedance of epoxy a very thin layer is used to avoid the extreme mismatch that results when used with common acousto-optic materials. Epoxy is generally satisfactory up to 150 MH_z. Beyond

150 MH_z other bonding methods must be used. Chang in chapter 4 of Ref. 39, presents an overview of current transducer bonding technology.

3. Acoustooptic Signal Processor

Practical Bragg cells are crystalline or glass material of cross section 1 cm^2 and approximately 15 cm long. Dimensions are chosen so as to meet the requirements of the design equations covered in the previous section. Signals input to the transducer are obtained from a wideband TRF receiver with tuning window equal to the acoustic frequency bandwidth. Laser light directed across the cell will be deflected to a position proportional to signal frequency with amplitude proportional to input signal strength. Modulation appearing on the signal will be preserved and output as sidebands of the carrier. Multiple frequencies will be processed without interference. The reader will note that there are no non-linear devices to create mixing products and that the phase gratings in the cell will correspond to the individual frequency inputs. Multiple signal handling without sweeping or time sharing is one of the major advantages of the acoustooptic receiver over other IFM receivers where multiple signals create ambiguity. In addition, the frequency resolution obtainable is limited only by the number of resolvable spots. Units with 500 spots have been achieved giving 1 part in 500 frequency measurement capability. Over a 500 MH_z bandwidth therefore, a 1 MH_z resolution is obtained. This is comparable to superheterodyne systems and much better than that typically attained by IFM's where a 5 MH_z resolutions is good. Figure 26 illustrates a basic acoustooptic receiver.

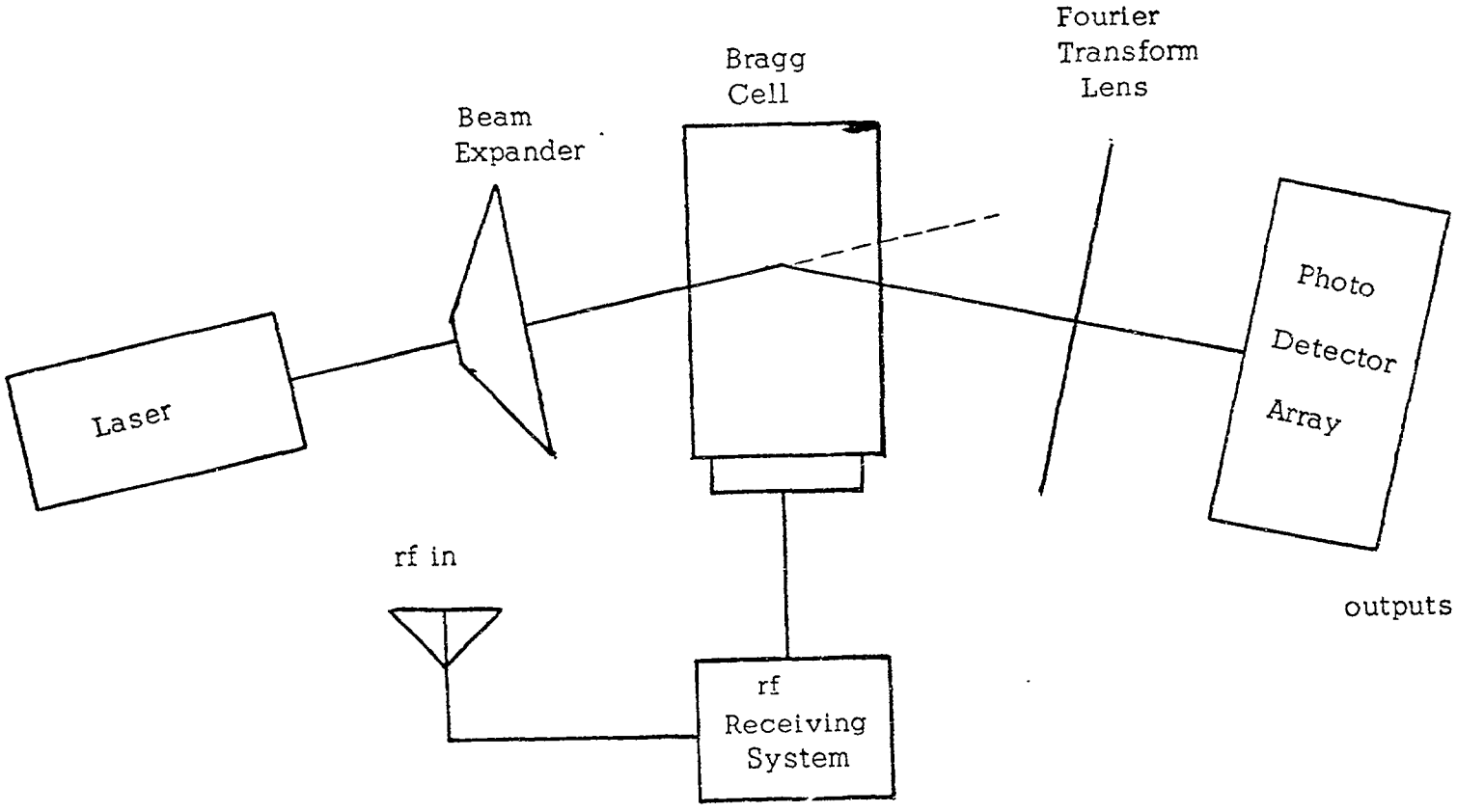

Figure 26. Practical Acoustooptic Receiver

The detector array could be a Reticon or Fairchild photodetector array using 500 photodetectors per unit. The output from each detector corresponds equivalently to a single channel of a multiple channel channelized receiver. Output signals from the detectors are video signals complete with modulation or pulse trains with pulse parameters intact except for the destructive influence to PW by the rise and fall time of the photodetector. The beam expander is used to illuminate the entire aperature while the Fourier transform lens resolves the signal beams as diffracted light in the frequency detector plane.

Displays for the detected outputs typically are direct laser beam display, film recording and multichannel photoelectric detectors. A visicorder or falling raster display unit can be used to combine frequency, pulse train analysis and obtain scan characteristics of radars in band.

The narrow bandwidth of the acoustooptic receiver can be overcome by applying the folded rf principle discussed in a previous section. The example given previously demonstrated the folding of multiple rf bands to a single channel 1000 MH_z wide. Using the same principle one can fold any band into the narrow acoustic bandwidth. Frequency resolution will be degraded by the number of times the frequency is downconverted and divided. For example, if the 1-2 GH_z band is folded to a 250 MH_z bandwidth, there is a one-to-four frequency relationship. Displayed outputs will represent four times the apparent frequency meaning that a signal covering 10 MH_z appears 2.5 MH_z wide. Acoustooptic

receiver sensitivity is no better than any other system with similar bandwidth. Sensitivity is set by the rf receiving system preceding the Bragg deflection device.

An acoustooptic receiver presently available is the Applied Technology 200-1 Instantaneous Fourier Transform receiver. The 200-1 features a 200 MH_z bandwidth with 1 MH_z resolution provided by 512 contiguous 400 KH_z channels.

The primary advantage in using the Bragg cell receiver is that all modulation types are preserved and detected by the receiver. Chirp radars, frequency agile emitters, pulsed signals, and CW signals will be detected without distortion. Simultaneous signals do not generate ambiguities since the device is linear and does not contain non-linear components prior to the photodetectors. Special purpose demodulators generally will not be necessary since most frequency deviations are greater than 400 KH_z and can be detected as they sweep through the contiguous channels.

VI. CONCLUSION

Factors that work to reduce POI can be overcome through efficient design. Noise factors are largely overcome by providing sufficient rf gain and low noise preamplifiers. Antenna and receiver scan rates of both transmitter and receiver can be overcome by properly selecting scan rates and antenna rotation speeds. Where system sensitivity is sufficient, non-scanning antennas and rapid frequency scan is found to maximize POI in scanning receivers. The effect of high density ECM environments is handled by providing means of reducing data input either by angle or frequency. Dedicated EW processors capable of handling extreme data rates provide near real-time signal analysis in dense environments. It is possible that in dense environments the processor will saturate causing a reduced POI. Buffering techniques and pulse sorting algorithms under development should alleviate the density problem. Wideband systems with unity POI possess limitations that must be overcome before widespread use is justified. The two-tuple receiver is expensive and cost ineffective compared to the standard microwave IFM. The IFM on the other hand is susceptible to interference by simultaneous pulses. Simultaneous pulse detectors that inhibit the IFM display are in use. However, in long term coincident situations such as dual-frequency CW radars, the display would be continually inhibited severely degrading the system POI. The acoustooptic receiver is the most attractive system except for limited

bandwidth. If increased bandwidth comes available the acoustooptic receiver could be a very important receiver for future ECM systems.

The need for IFM type receivers is questionable. Considering the ability of some signal processors to deinterleave signals and identify emitters without frequency information in a large percentage of intercepted signals. Signal ambiguity resolution on the remaining signals can be accomplished with a simple scanning receiver and at much less cost than an IFM receiver with polar display. Cost however will tend to stabilize since the system cost must include processor cost.

POI of unity is achievable when the factors presented are accounted for in the initial design. Determination of POI is quite straightforward with two methods available, mathematical and graphical. The graphical method was found easier to use and allows one to visualize system parameter effects on POI.

One will note that using scanning receivers and scanning intercept antennas against a scanning radar results in a near zero POI and a very long time to intercept. The ideal receiver is not currently available.

APPENDIX A

Define the total output temperature of a system, at temperature T, illustrated in Figure A-1 as

$$T_{out} = \alpha T_{in} + (1-\alpha) T \tag{A-1}$$

For the following calculation, assume all noise temperatures are referenced to the input of all devices (standard practice). T_{ext} is the actual external noise temperature input to the device. For simplification assume 290°K. Utilizing equation (A-1) T_{out} is determined as follows

$$T_{out} = T_o G_1 G_2 \alpha + T_1 G_1 G_2 \alpha + (1-\alpha) G_2 T + T_2 G_2 \tag{A-2}$$

Let F_e be the equivalent noise figure of the system where:

$$F_e = K T_{out} B / K T_o B G_1 G_2 \alpha = T_{out} / T_o G_1 G_2 \alpha \tag{A-3}$$

Where:

T_o = $T_{ext} = 290°K$

k = Boltzmann's constant

B = noise bandwidth of the device

T_1, T_2, T are the noise temperatures of blocks 1, 2, and the lossy element respectively.

F_1, F_2 are the noise figures of blocks 1 and 2 respectively

G_1, G_2 are the stage gains of blocks 1 and 2.

Substituting equation (A-2) into equation (A-3), one obtains:

$$F_e = \frac{1}{T_o}\left[T_o + T_1 + \frac{(1-\alpha)T}{G_1\alpha} + \frac{T_2}{G_2\alpha} \right] \qquad \text{(A-4)}$$

$$\simeq F_1 + \frac{(1-\alpha)T}{T_o G_1 \alpha} + \frac{F_2 - 1}{G_1\alpha} \qquad \text{(A-5)}$$

The equivalent noise figure is defined as:

$$F_e = \frac{T_e}{T_o} + 1 \qquad \text{or} \qquad T_e = (F_e - 1)\, T_o \qquad \text{(A-6)}$$

substituting equation (A-6) for F_e into equation (A-5) and multiplying by T_o,

$$T_e = T_o (F_1 - 1) + \frac{(1-\alpha)T}{G_1\alpha} + \frac{(F_2-1)\,T_o}{G_1\alpha} \qquad \text{(A-7)}$$

Noting that $T_o(F_1-1) = T_1$ and $T_o(F_2-1) = T_2$ equation (A-7) becomes:

$$T_e = T_1 + \frac{(1-\alpha)T}{G_1\alpha} + \frac{T_2}{G_1\alpha} \qquad \text{(A-8)}$$

Since $1/\alpha = L$,

$$T_e = T_1 + \frac{(L-1)T}{G_1} + \frac{LT_2}{G_1} \qquad \text{(A-9)}$$

If one allows G_1 to go to unity equation (A-9) becomes:

$$T_e = T_1 + (L-1)T + LT_2 \qquad \text{(A-10)}$$

Equation (A-10) is a more accurate version of equation (A-6).

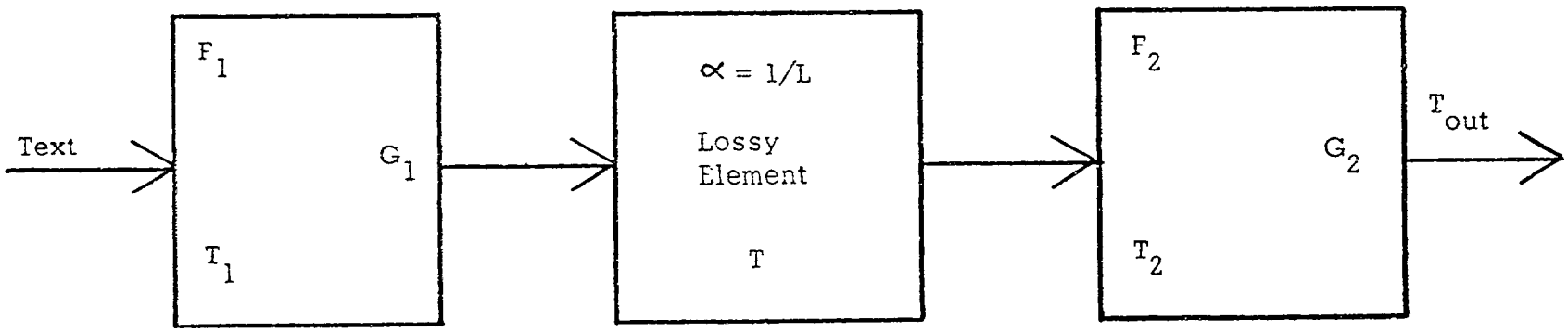

Figure A-1. Sample System with Lossy Element

APPENDIX B

J. B. Johnson's experiments demonstrated that the mean-square noise voltage in a band of frequencies (f_2 to f_1) which appears across the terminals of resistor R, is given by: [11]

$$\overline{e_n^2} = \int_{f_1}^{f_2} 4KTR\, df = 4KTR\Delta F \qquad \text{(B-1)}$$

For maximum power transfer consider a matched load [12] where:

$$\text{Power} = \frac{E^2}{4R_S} \qquad \text{(B-2)}$$

Where:

E = source voltage

R_S = source resistance

Using equation (B-1) and equation (B-2) the available noise power N is given by:

$$N = \frac{\overline{e_n^2}}{4R} = \frac{4KTR\Delta F}{4R} = KT\Delta F \qquad \text{(B-3)}$$

The noise figure of a device is simply defined as the ratio between input signal-to-noise ratio and output signal-to-noise ratio:

$$F = \frac{(S_i/N_i)}{(S_o/N_o)} = \frac{S_i N_o}{N_i S_o} \qquad \text{(B-4)}$$

Since $S_o = GS_i$ where G is the gain

$$F = \frac{S_i N_o}{N_i G S_i} = \frac{N_o}{N_i G} \tag{B-5}$$

The output noise power is the sum of the device noise, N_D, and the input noise times the gain, or:

$$N_o = N_D + G N_i \tag{B-6}$$

substituting equation (B-6) into equation (B-5):

$$F = \frac{G N_i + N_o}{N_i G} = 1 + \frac{N_D}{N_i G} \tag{B-7}$$

If the source and device are matched and the noise from the source is thermal and a result of a resistance at temperature T_o, the input noise is Johnson thermal noise.

$$F = 1 + \frac{N_D}{G K T_o \Delta f} \tag{B-8}$$

If one assumes that all noise generated internally can be considered as emanating from a single resistor at the input where the resistor is matched to the source, $N_D = GkT_e \Delta F$. Where T_e is equal to the equivalent noise temperature of the resistor. Substituting N_D into equation (B-7) one obtains

$$F = 1 + \frac{T_e}{T_o} \tag{B-9}$$

Using the approximate formula for noise power, $N = kTBF$, let $B = \Delta F$ and substitute equation (B-9) for F to obtain

$$N = K T_o \Delta f \left(1 + \frac{T_e}{T_o}\right) = K \Delta F (T_o + T_e) \tag{B-10}$$

From Johnson's exact noise power formula, equation (B-1) the actual noise at temperature T_e is given by:

$$N = k T_e \Delta F \tag{B-11}$$

The error involved in using the approximate equation is the ratio of the approximate noise power (equation (B-10))to the actual noise power (equation (B-11))

$$\text{Error} = \frac{K \Delta F (T_o + T_e)}{K \Delta F T_e} = 1 + \frac{T_o}{T_e} \tag{B-12}$$

Or in dB:

$$\text{Error (dB)} = 10 \log_{10} \left[1 + \frac{T_o}{T_e} \right] \tag{B-13}$$

To illustrate, assume a receiver with the following characteristics:

F = 4.5 dB (2.82)

B = ΔF = 100 KH_z

T_o = 290°K

From equation (A-11), $T_e = (F-1)T_o$, substituting for T_o, T_e = 528°K

Approximate sensitivity:

Sens = $kT_o \Delta F F = 1.13 \times 10^{-15}$ watts .... -119.5dBm

Exact sensitivity:

Sens = $kT_e \Delta F = 7.29 \times 10^{-16}$ watts ..... -121.4dBm

APPENDIX C

Gaussian noise is described by the probability distribution function

$$P(v,\phi)\,dv = \frac{1}{\sqrt{2\pi\psi_o}}\ \exp\left[-v^2/2\psi_o\right]\,dv \qquad \text{(C-1)}$$

where the phase ϕ is defined in reference 14, page 132. $P(v,\phi)$ is the probability of finding the noise voltage v between the values v and v+dv. ψ_o is the variance or mean-square value of the noise voltage, and it is assumed that the mean, $\bar{v}$ is zero. The probability density function of the noise envelope output from an envelope detector with an input of Gaussian noise is found by averaging over all phases, ϕ

$$P(R)\,dR = \int_0^{2\pi} P(R,\phi)\,d\phi \qquad \text{(C-2)}$$

where R is the amplitude function of the envelope detector and filter output. Carrying out the integration one obtains

$$P(R)\,dR = \frac{R}{\psi_o}\ \exp\left[-R^2/2\psi_o\right]\,dR \qquad \text{(C-3)}$$

Equation (C-3) is a form of the Rayleigh probability density function. [9,14] For an excellent discussion and complete derivation of the detection of signal in Gaussian noise the author refers the reader to Reich and Swerling. [15]

The probability that the envelope of the noise voltage is between v_1 and v_2 is given by

$$\text{PROB}\left[V_1 < R < V_2\right] = \int_{V_1}^{V_2} \frac{R}{\psi_o} \exp\left[-R^2/2\psi_o\right] dR \qquad \text{(C-4)}$$

It then follows that the probability that the noise envelope exceeds V_t is

$$\text{PROB}\left[V_t < R < \infty\right] = \int_{V_t}^{\infty} \frac{R}{\psi_o} \exp\left[-R^2/2\psi_o\right] dR \qquad \text{(C-5)}$$

where V_t is the receiver threshold voltage. Carrying out the integration yields the probability of false alarm, P_{fa}, given by

$$P_{fa} = \exp\left(-V_t^2/2\psi_o\right) \qquad \text{(C-6)}$$

APPENDIX D

When one considers signal plus Gaussian noise in an envelope detector, the output is given as

$$P_s(R)\,dR = \frac{R}{\psi_o} \exp\left(-\frac{R^2+A^2}{2\psi_o}\right) I_o\left(\frac{RA}{\psi_o}\right) \quad dR \tag{D-1}$$

where A is the amplitude of a sine wave input signal, and $I_o(z)$ is a modified Bessel function of zero order and argument z defined by

$$I_o(z) = \sum_{n=0}^{\infty} z^{2n}/2^{2n} n!\,n! \tag{D-2}$$

For Z large an asymptotic expansion of $I_o(z)$ is given by

$$I_o(z) \cong \frac{e^z}{\sqrt{2\pi z}} \left(1 + \frac{1}{8z} + \cdots\right) \tag{D-3}$$

The probability that the signal will exceed V_t is the probability of detection, P_d, given by

$$P_d = \int_{V_t}^{\infty} P_s(R)\,dR \tag{D-4}$$

where $P_s(R)$ is defined by equation (D-1). The evaluation of equation (D-4) must be made by numerical techniques or series approximation. A series approximation for P_d valid when $RA/\psi_o \gg 1$, $A \gg |R-A|$, and terms in A^{-3} and beyond can be neglected is

$$P_d = \frac{1}{2}\left(1 - \operatorname{erf}\frac{V_t - A}{\sqrt{2\psi_o}}\right) + \frac{\exp\left[-\frac{(V_t-A)^2}{2\psi_o}\right]}{2\sqrt{2\pi}\left(\frac{A}{\psi_o}\right)}\left[1 - \frac{V_T - A}{4A} + \frac{1 + (V_t-A)^2}{\frac{8A^2}{\psi_o}}\psi_o - \cdots\right] \quad \text{(D-5)}$$

where erf z is given by

$$\operatorname{erf} z = \frac{2}{\sqrt{\pi}} \int_0^z e^{-v^2}\, dv \quad \text{(D-6)}$$

APPENDIX E

From equations (A-5) and (A-12) and Figure 8, the total noise figure of the system can be written as

$$F_T = F_1 + \frac{(F_2 - 1)}{G_1} + \frac{(F_3 - 1)}{G_2 G_1} + \cdots\cdots \qquad \text{(E-1)}$$

where:

F_1 = noise figure of first stage

G_1 = gain of the first stage

L_1 = loss of the first stage

Consider now the contribution of each term. Since G_1 is a loss, one can consider $G_1 = L_1$. The rf amplifier contribution then becomes $L_1(F_2-1)$. The i-f system contribution must be reflected to the mixer stage. By substitution

$$\frac{(F_3 - 1)}{G_1 G_2} = \frac{L_1 (F_3 - 1)}{G_A} \qquad \text{(E-2)}$$

where G_A is the rf amplifier gain indicated in Figure 8. F_3 can be written to indicate the lossy effects of the filter that establishes maximum bandwidth (roofing filter) and the i-f amplifier gain. The noise figure of a mixer up to and including losses and the i-f noise figure is [21]

$$F_m = L_c (F_1 + t - 1) \qquad \text{(E-3)}$$

where:

F_m = mixer noise figure

L_c = mixer conversion loss

F_1 = first i-f noise figure

t = temperature ratio[1]

L_2, the noise contributed by the roofing filter degrades the i-f noise figure. The effects of L_2 are noted by inclusion in equation (E-3)

$$F_3 = F_m = L_c (L_2 + F_1 + t - 1) \tag{E-4}$$

By substituting $L_1=F_1$, $L_1=G_1$, equations (E-2), (E-3) and (E-4) into equation (E-1) F_T becomes

$$F_t = L_1 + L_1 (F_2 - 1) + \frac{L_1 (L_c (L_2 + F_1 + t - 1))}{G_A} + \ldots . \tag{E-5}$$

Equation (E-5) is the equation used to calculate effective receiver noise performance.

Confining gain can readily be calculated by assuming that only the first two stages affect noise figure. Therefore since $L_1=F_1$

$$F_T = F_1 + \frac{(F_2 - 1)}{G_1} \tag{E-6}$$

In order to consider noise confined to that generated by the first two stages

$$F_T - L_1 - L_1 (F_2 - 1) \gg \frac{L_1 (L_c (L_2 + F_1 + t - 1))}{G_A} \tag{E-7}$$

---

[1] Approximate unity for Schottky mixers. For other devices refer to "VHF Techniques", McGraw-Hill, Vol. II, p. 802.

Define confining gain, G_c as

$$G_c = 10 \frac{L_1 (L_c (L_2 + F_1 + t - 1))}{F_T - L_1 - L_1 (F_2 - 1)} \qquad \text{(E-8)}$$

The factor of ten is simply an engineering approximation that guarantees the validity of equation (E-8).

LIST OF REFERENCES

1. Boyd, J. A., and others, Electronic Countermeasures, Institute of Science and Technology of the University of Michigan, 1961.

2. DELETED.

3. "Editor", "What's New in ELINT Receiving Hardware?", Electronic Warfare, p. 19-25, July/August 1974.

4. Richards, P. I., "Probability of Coincidence for Two Periodically Recurring Events", Annals of Mathematical Statistics, V. 19, No. 1, March 1948.

5. Cuccia, C. L., Gill, W. J., Wilson, L. H., "Sensitivity of Microwave Earth Stations for Analog and Digital Communications", Electronics, p. 47-54, January 1969.

6. DiFranco, J. V., Rubin, W. L., Radar Detection, Prentice-Hall, 1968.

7. Reference Data for Radio Engineers, 5th Ed., Ch. 27, International Telephone and Telegraph Corporation, 1973.

8. Sylvania Electronics Defense Laboratories Report EDL-M658, Receiver System Noise Study, by W. F. Oliver, 27 March 1964.

9. Skolnik, M. I., Radar Systems, McGraw-Hill, 1962.

10. Baker, W., "Obtain the Correct Dope on Receiver Sensitivity", Microwaves, p. 50-51, February 1969.

11. Johnson, J. B., "Thermal Agitation of Electricity in Conductors", Physics Review, V. 32, p. 97-109, July 1928.

12. Strum, R. D., Ward, J. R., Electronic Circuits and Networks, p. 300, Quantum Publishers, 1973.

13. Taub, H., Schilling, D. L., Principles of Communication Syste..., p. 253, McGraw-Hill, 1971.

14. Stein, S., Jones, J. J., Modern Communication Principles, p. 136-145, McGraw-Hill, 1967.

15. Reich, E., Swerling, P., "The Detection of a Sine Wave in Gaussian Noise", Journal of Applied Physics, V. 24, No. 3, p. 289-296, March 1953.

16. Davenport, W. B., Jr., Probability and Random Processes, p. 92-136, McGraw-Hill, 1970.

17. Barton, D. F., and others, Modern Radar, p. 90-92, Wiley, 1965.

18. Nicholson, J. E., "The Needle in the Haystack", Electronic Warfare, p. 81, January 1974.

19. Larson, H. J., Introduction to Probability and Statistical Inference, p. 47, Wiley, 1969.

20. Urkowitz, H., "Energy Detection of Unknown Deterministic Signals", Proceedings of the IEEE, V. 55, No. 4, p. 523-531, April 1967.

21. Lipsky, S. E., "Calculate the Effects of Noise on ECM Receivers", Microwaves, p. 65-71, October 1974.

22. Stanford Electronics Laboratory Report 150-3, Characteristics of Crystal Video Receivers Employing Rf Preamplification, by W. E. Ayer.

23. Klipper, H., "Sensitivity of Crystal Video Receivers with Rf Preamplification", Microwave Journal, V. 8, No. 8, August 1965.

24. Operations Evaluations Group, Office of the Chief of Naval Operations Report OEG-Study 294, Design of Shipborne Search Receivers.

25. Schlesinger, R. J., and others, Principles of Electronic Warfare, p. 56-77, Prentice-Hall, 1961.

26. Watkins-Johnson Company, WJ-940 Receiving System Technical Data, February 1975.

27. Watkins-Johnson Company, WJ-1007 Microwave Collection System Technical Specifications.

28. DELETED.

29. Stanford Research Institute Report, The Microscan Signal Intercept and Analysis System, by H. S. Hewitt, April 1970.

30. Keenly, R. R., "New Systems Concepts for Increased ELINT Intercept", Electronic Warfare, p. 63-68, February 1973.

31. Editor, "Pointer-New Concept in Digital Radar Warning", Electronic Warfare, p. 57-60, November 1973.

32. Tuite, D. F., "Comparing ECM Antennas: Horns vs. Spirals", Microwaves, p. 44-50, October 1972.

33. Editor, "World's First EW Minicomputer Debuts", Electronic Warfare, p. 68-75, September 1973.

34. Stanford Electronics Laboratories Technical Report No. 1905-2/1709-3, SU-SEL-68-013, Theory of Polar-Display Signal Analyzers, and a Radio Direction-Finding Analogy, by G. A. Myers, March 1968.

35. Spitzer, N. J., Experimental Evaluation of a Linear-Polar-Display Signal Analyzer, Master's Degree Thesis, United States Naval Postgraduate School, Monterey, California, 1969.

36. DELETED.

37. Editor, "Multi-Mode ELINT Receiver Developed", Electronic Warfare, p. 59-62, April 1973.

38. Uchida, N., Niizeki, N., "Acoustooptic Deflection Materials and Techniques", Proceedings of the IEEE, V. 61, No. 8, p. 1073-1092, 8 August 1973.

39. Chang, I. C., Acousto-optic Devices and Applications, paper written for Applied Technology, Sunnyvale, California, 1975.

40. Heynau, H. A. "The State of the Art in Beam Steering and Control Using Acousto-optics", Acoustic Surface Wave and Acousto-optic Device, V. 4, p. 127-138, Optosonic Press, 1971.

INITIAL DISTRIBUTION LIST

		No. Copies
1.	Defense Documentation Center Cameron Station Alexandria, Virginia 22314	2
2.	Library, Code 0212 Naval Postgraduate School Monterey, California 93940	2
3.	Dr. Stephen Jauregui, Jr., Code 52Ja Associate Professor of Electronics Department of Electrical Engineering Naval Postgraduate School Monterey, California 93940	10
4.	Department Chairman, Code 52 Department of Electrical Engineering Naval Postgraduate School Monterey, California 93940	1
5.	LT Barry F. Schwoerer, USN AITANTISUBRON THIRTY-EIGHT (VS-38) Naval Air Station, North Island San Diego, California 92135	2
6.	Dr. Richard Adler, Code 52Ab Assistant Professor of Electrical Engineering Department of Electrical Engineering Naval Postgraduate School Monterey, California 93940	1
7.	Dean of Research Naval Postgraduate School Monterey, California 93940	1
8.	Commander Naval Electronics Systems Command (PME-107 Navy Department Washington, D. C. 20360 Attn: P. Lowell	1

		No. Copies
9.	Commander Naval Electronics Systems Command (PME-107) Navy Department Washington, D. C. 20360 Attn: LCDR R. Todaro	1
10.	Commander Naval Electronics Systems Command (PME-107) Navy Department Washington, D. C. 20360 Attn: R. Materazza	2
11.	Commander Naval Security Group Command (G-82) Navy Security Group Headquarters 3801 Nebraska Ave., N. W. Washington, D. C. 20360 Attn: LCDR F. Cleary	1
12.	Commander Naval Security Group Command (G-82) Navy Security Group Headquarters 3801 Nebraska Ave., N. W. Washington, D. C. 20360 Attn: CDR H. Schoemaker	1